
CHAPTER 2

HEAT TRANSFER APPLICATIONS IN BIOLOGICAL SYSTEMS

Liang Zhu

University of Maryland Baltimore County, Baltimore, Maryland

2.1 INTRODUCTION	33
2.2 FUNDAMENTAL ASPECTS OF BIOHEAT TRANSFER	33
2.3 BIOHEAT TRANSFER MODELING	36

2.4 TEMPERATURE, THERMAL PROPERTY, AND BLOOD FLOW MEASUREMENTS	46
2.5 HYPERTHERMIA TREATMENT FOR CANCERS AND TUMORS	53
REFERENCES	62

2.1 INTRODUCTION

Over the past 100 years, the understanding of thermal and mechanical properties of human tissues and physics that governs biological processes has been greatly advanced by the utilization of fundamental engineering principles in the analysis of many heat and mass transport applications in biology and medicine. During the past two decades, there has been an increasingly intense interest in bioheat transfer phenomena, with particular emphasis on therapeutic and diagnostic applications. Relying on advanced computational techniques, the development of complex mathematical models has greatly enhanced our ability to analyze various types of bioheat transfer process. The collaborations among physiologists, clinicians, and engineers in the bioheat transfer field have resulted in improvements in prevention, treatment, preservation, and protection techniques for biological systems, including use of heat or cold treatments to destroy tumors and to improve patients' outcome after brain injury, and the protection of humans from extreme environmental conditions.

In this chapter we start with fundamental aspects of local blood tissue thermal interaction. Discussions on how the blood effect is modeled in tissue then follow. Different approaches for theoretically modeling the blood flow in the tissue are shown. In particular the assumptions and validity of several widely used continuum bioheat transfer equations are evaluated. Different techniques to measure temperature, thermophysical properties, and blood flow in biological systems are then described. The final part of the chapter focuses on one of the medical applications of heat transfer, hyperthermia treatment for tumors.

2.2 FUNDAMENTAL ASPECTS OF BIOHEAT TRANSFER

One of the remarkable features of the human thermoregulatory system is that we can maintain a core temperature near 37°C over a wide range of environmental conditions and during thermal stress. The value of blood flow to the body varies over a wide range, depending upon the need for its three primary functions:

1. Mass transfer in support of body metabolisms. Blood transports oxygen to the rest of the body and transports carbon dioxide and other waste from the cells.
2. Regulation of systemic blood pressure. The vascular system is a primary effector in the regulation of systemic blood pressure through its ability to alter the distribution of blood flow and regulate the cardiac output and thereby buffer systemic pressure fluctuations.
3. Heat transfer for systemic thermoregulation.

As for the third primary function, blood is known to have a dual influence on the thermal energy balance. First it can be a heat source or sink, depending on the local tissue temperature. During wintertime, blood is transported from the heart to warm the rest of the body. On the other hand, during hyperthermia treatment for certain diseases where the tissue temperature is elevated to as high as 45°C by external devices, the relatively cold blood forms cold tracks that can decrease the treatment efficacy. The second influence of the blood flow is that it can enhance heat dissipation from the inside of the body to the environment to maintain a normal body temperature. Theoretical study has shown that if the heat produced in the central areas of the body at rest condition could escape only by tissue conduction, the body temperature would not reach a steady state until it was about 80°C. A lethal temperature would be reached in only 3 hours. During exercise, our body temperature would have typically risen 12°C in 1 hour if no heat were lost by blood flow. Maintaining a core temperature of 37°C during thermal stress or exercise in the body is achieved by increasing the cardiac output by central and local thermoregulation, redistributing heat via the blood flow from the muscle tissue to the skin, and speeding the heat loss to the environment by evaporation of sweat.

Thermal interaction between blood and tissue can be studied either experimentally or theoretically. However, for the following reasons it is difficult to evaluate heat transfer in a biological system:

- The complexity of the vasculature. It is not practical to develop a comprehensive model that includes the effect of all thermally significant vessels in a tissue. Therefore, the most unusual and difficult basic problem of estimating heat transfer in living biologic systems is modeling the effect of blood circulation.
- Temperature response of the vasculature to external and internal effects is also a complex task. In a living system, the blood flow rate and the vessel size may change as a response to local temperature, local pH value, and the concentration of local O₂ and CO₂ levels.
- The small thermal length scale involved in the microvasculature. Thermally significant blood vessels are generally in a thermal scale of less than 300 μm. It has been difficult to build temperature-measuring devices with sufficient resolution to measure temperature fluctuation.

For the above reasons, even if the heat transfer function of the vascular system has been appreciated since the mid-nineteenth century, only in the past two decades, has there been a revolution in our understanding of how temperature is controlled at the local level, both in how local microvascular blood flow controls the local temperature field and how the local tissue temperature regulates local blood flow.

Until 1980, it was believed that, like gaseous transport, heat transfer took place in the capillaries because of their large exchange surface area. Several theoretical and experimental studies (Chato, 1980; Chen and Holmes, 1980; Weinbaum et al., 1984; Lemons et al., 1987) have been performed to illustrate how individual vessels participate in local heat transfer, and thus to understand where the actual heat transfer between blood and tissue occurs. In these analyses, the concept of thermal equilibration length was introduced. Thermal equilibration length of an individual blood vessel was defined as a distance over which the temperature difference between blood and tissue drops a certain percentage. For example, if the axial variation of the tissue and blood temperature difference can be expressed as $\Delta T = \Delta T_0 e^{-x/L}$, where ΔT_0 is the temperature difference at the vessel entrance, and L and $4.6L$ are the thermal equilibration lengths over which ΔT decreases to 37 percent and 1 percent, respectively, of its value at the entrance. Blood vessels whose thermal equilibration length is comparable to their physical length are considered thermally significant.

Chato (1980) first theoretically investigated the heat transfer from individual blood vessels in three configurations: a single vessel, two vessels in counterflow, and a single vessel near the skin surface. It was shown that the Graetz number, proportional to the blood flow velocity and radius, is the controlling parameter determining the thermal equilibration between the blood and tissue. For blood vessels with very low Graetz number, blood quickly reaches the tissue temperature. It was also demonstrated that heat transfer between the countercurrent artery and vein is affected by the vessel center-to-center spacing and mass transport between them.

In an anatomic study performed on rabbit limbs, Weinbaum et al. (1984) identified three vascular layers (deep, intermediate, and cutaneous) in the outer 1-cm tissue layer. Subsequently, three fundamental vascular structures were derived from the anatomic observation: (1) an isolated vessel embedded in a tissue cylinder, as shown by the intermediate tissue layer; (2) a large artery and its countercurrent vein oriented obliquely to the skin surface, as shown in the deep tissue layer; and (3) a vessel or vessel pair running parallel to the skin surface in the cutaneous plexus. These three vascular structures served as the basic heat transfer units in the thermal equilibration analysis in Weinbaum et al. (1984).

As shown in Weinbaum et al. (1984), 99 percent thermal equilibration length of a single blood vessel embedded in a tissue cylinder was derived as

$$x_{cr} = 1.15aPrRe[0.75 + K\ln(R/a)] \quad (2.1)$$

where a and R are the blood vessel and tissue cylinder radii, respectively; Pr and Re are the blood flow Prandtl number and Reynolds number, respectively; and K is the ratio of blood conductivity to tissue conductivity. It is evident that x_{cr} is proportional to the blood vessel size and its blood flow velocity. Substituting the measured vascular geometry and the corresponding blood flow rate number for different blood vessel generations (sizes) from a 13-kg dog (Whitmore, 1968), one could calculate the thermal equilibration length as listed in Table 2.1.

Several conclusions were drawn from the comparison between x_{cr} and L . In contrast to previous assumptions that heat transfer occurs in the capillary bed, for blood vessels smaller than 50 μm in diameter, blood quickly reaches the tissue temperature; thus, all blood-tissue heat transfer must have already occurred before entering into these vessels. For blood vessels larger than 300 μm in diameter, there is little change in blood temperature in the axial direction because of their much longer thermal equilibration length compared with the vessel length. The medium-sized vessels between 50 and 300 μm in diameter are considered thermally significant because of their comparable thermal equilibration length and physical length. Those blood vessels are primary contributors to tissue heat transfer. Note that the conclusions are similar to that drawn by Chato (1980).

The most important aspect of the bioheat transfer analysis by Weinbaum and coinvestigators was the identification of the importance of countercurrent heat transfer between closely spaced, paired arteries and veins. The countercurrent heat exchange mechanism, if dominant, was suggested as an energy conservation means since it provides a direct heat transfer path between the vessels. It was observed that virtually all the thermally significant vessels (>50 μm in diameter) in the skeletal

TABLE 2.1 Thermal Equilibration Length in a Single Vessel Embedded in a Tissue Cylinder

Vessel radius a , mm	Vessel length L , cm	R/a	x_{cr} , cm
300	1.0	30	9.5
100	0.5	20	0.207
50	0.2	10	0.014
20	0.1	7	0.0006

muscle were closely juxtaposed artery-vein pairs (Weinbaum et al., 1984). Thermal equilibration in the artery (approximately 50 to 300 μm in diameter) in a countercurrent pair was estimated based on a simple heat conduction analysis in the cross-sectional plane. It was noted that the thermal equilibration length in the countercurrent artery was at least 3 times shorter than that in a single vessel of the same size embedded in a tissue cylinder (Weinbaum et al., 1984). Significantly, short thermal equilibration length in comparison with that of a single vessel suggests that the primary blood tissue heat exchange mechanism for vessels larger than 50 μm in the deep layer is the incomplete countercurrent heat exchange. Therefore, for modeling heat transfer in these tissue regions, reasonable assumptions related to the countercurrent heat exchange mechanism can be made to simplify the mathematical formulation.

Theoretical analysis of the thermal equilibration in a large vessel in the cutaneous layer (Chato, 1980; Weinbaum et al., 1984) demonstrated that its thermal equilibration length was much longer than its physical length during normal and hyperemic conditions despite the close distance from the skin surface. It was suggested that the large vessels in the cutaneous layer can be far from thermal equilibration and are, therefore, capable of delivering warm blood from the deep tissue to the skin layer. This superficial warm blood shunting is very important in increasing the normal temperature gradient at the skin surface and, therefore, plays an important role in losing heat during heavy exercise. On the contrary, during surface cooling there is rapid cutaneous vasoconstriction in the skin. The minimally perfused skin, along with the underlying subcutaneous fat, provides a layer of insulation, and the temperature gradient from the skin surface into the muscle becomes almost linear (Bazett, 1941) yielding the lowest possible heat transfer from the body.

2.3 BIOHEAT TRANSFER MODELING

The effects of blood flow on heat transfer in living tissue have been examined for more than a century, dating back to the experimental studies of Bernard in 1876. Since then, mathematical modeling of the complex thermal interaction between the vasculature and tissue has been a topic of interest for numerous physiologists, physicians, and engineers. A major problem for theoretical prediction of temperature distribution in tissue is the assessment of the effect of blood circulation, which is the dominant mode of heat removal and an important cause of tissue temperature inhomogeneity.

Because of the complexity of the vascular geometry, there are two theoretical approaches describing the effect of blood flow in a biological system. Each approach represents two length scales over which temperature variations may occur.

- Continuum models, in which the effect of blood flow in the region of interest is averaged over a control volume. Thus, in the considered tissue region, there is no blood vessel present; however, its effect is treated by either adding an additional term in the conduction equation for the tissue or changing some of the thermophysical parameters in the conduction equation. The continuum models are simple to use since the detailed vascular geometry of the considered tissue region need not be known as long as one or two representative parameters related to the blood flow are available. The shortcoming of the continuum model is that since the blood vessels disappear, no point-by-point variation in the blood temperature is available. Another shortcoming is associated with the assumptions introduced when the continuum model was derived. For different tissue regions and physiological conditions, these assumptions may not be valid.
- Vascular models, in which blood vessels are represented as tubes buried in tissue. Because of the complicate vascular geometry one may only consider several blood vessels and neglect the others. Recent studies (Dorr and Hynynen, 1992; Crezee and Lagendijk, 1990; Roemer, 1990) have demonstrated that blood flow in large, thermally unequilibrated vessels is the main cause for temperature nonhomogeneity during hyperthermia treatment. Large blood vessels may significantly cool tissue volumes around them, making it very difficult to cover the whole tumor volume with

therapeutic thermal exposure. In applications where point-to-point temperature nonuniformities are important, vascular model has been proved to be necessary to predict accurately the tissue temperature field (Zhu et al., 1996a). In recent years, with the breakthrough of advanced computational techniques and resources, vascular models (Raaymakers et al., 2000) for simulating vascular networks have grown rapidly and already demonstrated its great potential in accurate and point-to-point blood and tissue temperature mapping.

2.3.1 Continuum Models

In continuum models, blood vessels are not modeled individually. Instead, the traditional heat conduction equation for the tissue region is modified by either adding an additional term or altering some of the key parameters. The modification is relatively simple and is closely related to the local vasculature and blood perfusion. Even if the continuum models cannot describe the point-by-point temperature variations in the vicinity of larger blood vessels, they are easy to use and allow the manipulation of one or several free parameters. Thus, they have much wider applications than the vascular models. In the following sections, some of the widely used continuum models are introduced and their validity is evaluated on the basis of the fundamental heat transfer aspects.

Pennes Bioheat Transfer Model. It is known that one of the primary functions of blood flow in a biological system is the ability to heat or cool the tissue, depending on the relative local tissue temperature. The existence of a temperature difference between the blood and tissue is taken as evidence of its function to remove or release heat. On the basis of this speculation, Pennes (1948) proposed his famous heat transfer model, which is called Pennes bioheat equation. Pennes suggested that the effect of blood flow in the tissue be modeled as a heat source or sink term added to the traditional heat conduction equation. The Pennes bioheat equation is given by

$$\rho C \frac{\partial T_t}{\partial t} = k_t \nabla^2 T_t + q_{\text{blood}} + q_m \quad (2.2)$$

where q_m is the metabolic heat generation in the tissue, and the second term (q_{blood}) on the right side of the equation takes into account the contribution of blood flow to the local tissue temperature distribution. The strength of the perfusion source term can be derived as follows.

Figure 2.1 shows a schematic diagram of a small tissue volume perfused by a single artery and vein pair. The tissue region is perfused via a capillary network bifurcating from the transverse arterioles, and the blood is drained by the transverse venules. If one assumes that both the artery and vein keep a constant temperature when they pass through this tissue region, the total heat released is equal to the total amount of blood perfusing this tissue volume per second q multiplied by its density ρ_b , specific heat C_b , and the temperature difference between the artery and vein, and is given by

$$q \rho_b C_b (T_a - T_v) = (Q_{\text{in}} - Q_{\text{out}}) \rho_b C_b (T_a - T_v) \quad (2.3)$$

The volumetric heat generation rate q_{blood} defined as the heat generation rate per unit tissue volume, is then derived as

$$q_{\text{blood}} = [(Q_{\text{in}} - Q_{\text{out}})/V] \rho_b C_b (T_a - T_v) = \omega \rho_b C_b (T_a - T_v) \quad (2.4)$$

where ω is defined as the amount of blood perfused per unit volume tissue per second.

Note that both T_a and T_v in Eq. (2.4) are unknown. Applying the analogy with gaseous exchange in living tissue, Pennes believed that heat transfer occurred in the capillaries because of their large area for heat exchange. Thus, the local arterial temperature T_a could be assumed as a constant and equal to the body core temperature T_c . As for the local venous blood, it seems reasonable to assume that it equilibrates with the tissue in the capillary and enters the venules at the local tissue temperature.

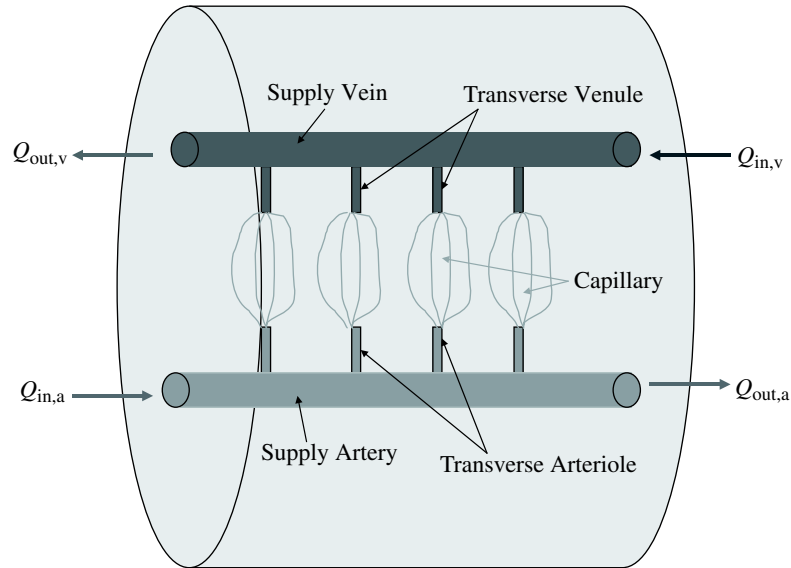


FIGURE 2.1 Schematic diagram of a tissue volume perfused by a single artery and vein pair.

Then the Pennes bioheat equation becomes

$$\rho C \frac{\partial T_t}{\partial t} = k_t \nabla^2 T_t + \omega \rho_b C_b (T_c - T_t) + q_m \quad (2.5)$$

This is a partial differential equation for the tissue temperature. As long as an appropriate initial condition and boundary conditions are prescribed, the transient and steady-state temperature field in the tissue can be determined.

The limitations of the Pennes equation come from the basic assumptions introduced in this model. First, it is assumed that the temperature of the arterial blood does not change when it travels from the heart to the capillary bed. As shown in Sec. 2.2, small temperature variations occur only in blood vessels with a diameter larger than 300 μm . Another assumption is that the venous blood temperature is approximated by the local tissue temperature. This is valid only for blood vessels with a diameter smaller than 50 μm . Thus, without considering the thermal equilibration in the artery and vein in different vessel generations, the Pennes perfusion source term obviously overestimates the effect of blood perfusion. To accurately model the effect of blood perfusion, the temperature variation along the artery and the heat recaptured by the countercurrent vein must be taken into consideration.

Despite the limitations of the Pennes bioheat equation, reasonable agreement between theory and experiment has been obtained for the measured temperature profiles in perfused tissue subject to various heating protocols. This equation is relatively easy to use, and it allows the manipulation of two blood-related parameters, the volumetric perfusion rate and the local arterial temperature, to modify the results. Pennes performed a series of experimental studies to validate his model. Over the years, the validity of the Pennes bioheat equation has been largely based on macroscopic thermal clearance measurements in which the adjustable free parameter in the theory, the blood perfusion rate (Xu and Anderson, 1999) was chosen to provide a reasonable agreement with experiments for the temperature decay in the vicinity of a thermistor bead probe. Indeed, if the limitation of Pennes bioheat equation is an inaccurate estimation of the strength of the perfusion source term, an adjustable blood perfusion rate will overcome its limitations and provide a reasonable agreement between experiment and theory.

Weinbaum-Jiji Bioheat Equation. Since 1980, researchers (Chato, 1980; Chen and Holmes, 1980; Weinbaum et al., 1984) have begun to question the validity of the Pennes bioheat equation. Later, Weinbaum and Jiji (1985) developed a new equation for microvascular blood tissue heat transfer, based on an anatomic analysis (Weinbaum et al., 1984) to illustrate that the predominant mode of heat transfer in the tissue was the countercurrent heat exchange between a thermally significant artery and vein pair. The near-perfect countercurrent heat exchange mechanism implies that most of the heat leaving the artery is transferred to its countercurrent vein rather than released to the surrounding tissue. Once there is a tissue temperature gradient along the countercurrent vessel axes, the artery and vein will transfer a different amount of energy across a plane perpendicular to their axes even if there is no net mass flow. This gives rise to a net energy transfer that is equivalent to an enhancement in tissue conductivity in the axial direction of the vessels. In the Weinbaum-Jiji bioheat equation, the thermal effect of the blood perfusion is described by an enhancement in thermal conductivity k_{eff} appearing in the traditional heat conduction equation,

$$\rho C \frac{\partial T}{\partial t} = k_{\text{eff}} \nabla^2 T_t + q_m \quad k_{\text{eff}} = k_t [1 + f(\omega)] \quad (2.6)$$

It was shown that k_{eff} is a function of the local blood perfusion rate and local vascular geometry.

The main limitations of the Weinbaum-Jiji bioheat equation are associated with the importance of the countercurrent heat exchange. It was derived to describe heat transfer in peripheral tissue only, where its fundamental assumptions are most applicable. In tissue area containing a big blood vessel (>200 μm in diameter), the assumption that most of the heat leaving the artery is recaptured by its countercurrent vein could be violated; thus, it is not an accurate model to predict the temperature field. In addition, this theory was primarily developed for closely paired microvessels in muscle tissue, which may not always be the main vascular structure in other tissues, such as the renal cortex. Furthermore, unlike the Pennes bioheat equation, which requires only the value of local blood perfusion rate, the estimation of the enhancement in thermal conductivity requires that detailed anatomical studies be performed to estimate the vessel number density, size, and artery-vein spacing for each vessel generation, as well as the blood perfusion rate (Zhu et al., 1995). These anatomic data are normally not available for most blood vessels in the thermally significant range.

A New Modified Bioheat Equation. The Pennes and Weinbaum-Jiji models represent two extreme situations of blood-vessel thermal interaction. In the original Pennes model, the arterial blood releases all of its heat to the surrounding tissue in the capillaries and there is no venous rewarming. Pennes did not realize that thermal equilibration was achieved in vessels at least an order of magnitude larger than the capillaries. In contrast, in the Weinbaum-Jiji model the partial countercurrent rewarming is assumed to be the main mechanism for blood-tissue heat transfer. The derivation of the Weinbaum-Jiji equation is based on the assumption that heat transfer between the artery and the vein does not depart significantly from a perfect countercurrent heat exchanger. In other words, most of the heat lost by the artery is recaptured by its countercurrent vein rather than lost to the surrounding tissue. Subsequent theoretical and experimental studies have shown that this is a valid assumption only for vessels less than 200 μm diameter (Charny et al., 1990; Zhu et al., 1996a).

Several theoretical studies have suggested that one way to overcome the shortcomings of both models was to introduce a "correction coefficient" in the Pennes perfusion term (Chato, 1980; Baish, 1994; Brinck and Werner, 1994; Weinbaum et al., 1997; Zhu et al., 2002). In 1997, Weinbaum and coworkers (Weinbaum et al., 1997) modified the Pennes source term on the basis of the thermal analysis of a basic heat transfer unit of muscle tissue, a 1-mm-diameter tissue cylinder containing blood vessels smaller than 200 μm in diameter, as shown in Fig. 2.2. The countercurrent heat exchange between the s artery and vein defined in the anatomical studies of Myrhage and Eriksson (1984) led to the estimation of the heat loss recaptured by the s vein. The strength of the source term was then rederived taking into account the rewarming of the countercurrent venous blood in the s tissue cylinder. The thermal equilibration analysis on the countercurrent s artery and vein in the tissue

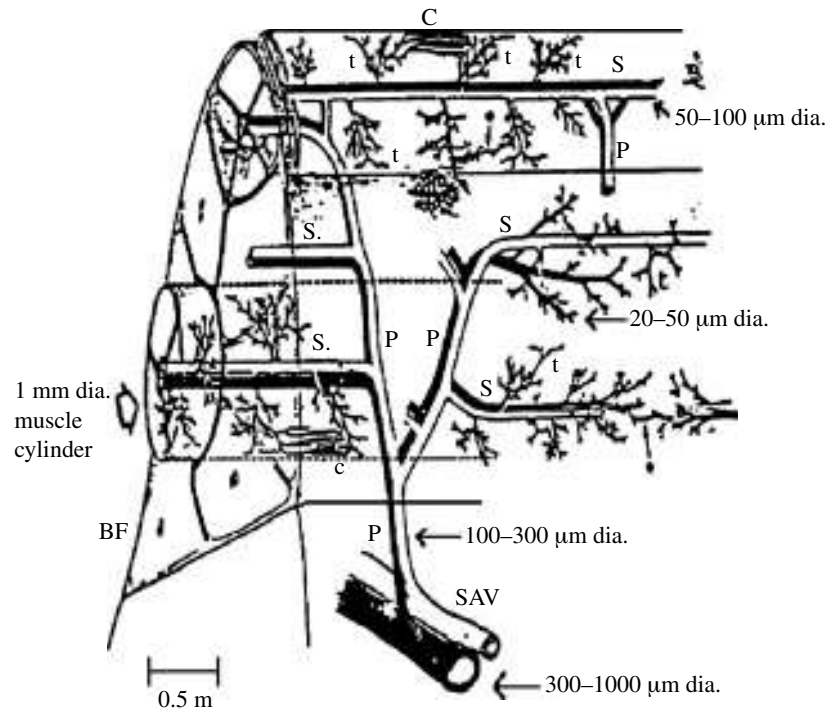


FIGURE 2.2 Macro- and microvascular arrangement in skeletal muscle. The blood supply for the muscle tissue cylinder comes from a branching countercurrent network of supply vessels. The primary (*P*) vessels originating from the SAV vessels, run obliquely across the muscle tissue cylinders and then branch into the long secondary (*s*) vessels. [From Myrhaage and Eriksson (1984), with permission.]

cylinder led to the following bioheat transfer equation:

$$\rho C \frac{\partial T_t}{\partial t} = k_t \nabla^2 T_t + \varepsilon \omega \rho_b C_b (T_{a0} - T_t) + q_m \quad (2.7)$$

Note that the only modification to the Pennes model is a correction coefficient in the Pennes source term. This correction coefficient can be viewed as a weighting function to correct the overestimation of the original Pennes perfusion term. An easy-to-use closed-form analytic expression was derived for this coefficient that depends on the vessel spacing and radius. From the anatomic studies of the vascular arrangements of various skeletal muscles, the correction coefficient was found to vary from 0.6 to 0.8 under normal physiological conditions, indicating that there is a 20 to 40 percent rewarming of the countercurrent vein. Note that it is close to neither unity (the Pennes model) nor zero (the Weinbaum-Jiji model). Thus, both the Pennes and Weinbaum-Jiji bioheat equations are not valid for most muscle tissue. Furthermore, as shown in Zhu et al. (2002), the arterial temperature T_{a0} may not be approximated as the body core temperature either, unless the local blood perfusion is very high. In most physiological conditions, it is a function of the tissue depth, blood vessel bifurcation pattern, and the local blood perfusion rate.

2.3.2 Experimental and Theoretical Studies to Validate the Models

Pennes (1948) performed a series of experimental studies to validate his model. He inserted and pulled thermocouples through the arms of nine male subjects to measure the radial temperature

profiles. He also measured the skin temperature distributions along the axis of the upper limb, as well as around the circumference of the forearm. Pennes then modeled the arm as a long cylinder and calculated the steady-state radial temperature profile. In this theoretical prediction, since the blood perfusion rate ω could not be directly measured, Pennes adjusted this parameter in his model to fit the solution to his experimental data for a fixed, representative ambient temperature and metabolic heating rate. The fitted value of blood perfusion rate ω was found to be between 1.2 and 1.8 mL blood/min/100 g tissue, which is a typical range of values for resting human skeletal muscle. Recently, Wissler (1998) reevaluated Pennes' original paper and analyzed his data. He found that the theoretical prediction agrees very well with Pennes' experimental results if the data were analyzed in a more rigorous manner.

Profound understanding of the heat transfer site and the countercurrent heat exchange between paired significant vessels was gained through the experiments (Lemons et al., 1987) performed on rabbit thigh to measure the transverse tissue temperature profiles in the rabbit thigh using fine thermocouples. The experimental study was designed to achieve two objectives. The first is to examine whether there exists detectable temperature difference between tissue and blood for different-size vessels. Existing detectable blood-tissue temperature difference implies that blood has not reached thermal equilibration with the surrounding tissue. The second is to examine the temperature difference between the countercurrent artery and vein. If the countercurrent heat exchange is dominant in blood tissue heat transfer, the vein must recapture most of the heat leaving the artery; thus, the temperature difference between the countercurrent artery and vein should not vary significantly in the axial direction.

Experimental measurements (Lemons et al., 1987) revealed small temperature fluctuations of up to 0.5°C in the deep tissue. The irregularities in the tissue temperature profiles were closely associated with the existence of blood vessels in the vicinity of the thermocouple wire. It was shown that temperature fluctuation was observed in all the blood vessels larger than 500 μm , in 67 percent of the vessels between 300 and 500 μm , and in 9 percent of the vessels between 100 and 300 μm . No temperature fluctuation was observed in blood vessels less than 100 μm in diameter. This finding indicates that the assumption in the Pennes model that arterial blood reaches the capillary circulation without significant prior thermal equilibration is inaccurate for this vascular architecture, and thus most of the significant blood-tissue heat transfer occurs in the larger vessels upstream. It was also observed that the temperature field rarely exceeded 0.2°C in any countercurrent pair, even when the difference in temperature between the skin and the central part of the rabbit thigh exceeded 10°C. This implies the effectiveness of the countercurrent heat exchange process throughout the vascular tree.

Similar experiments were performed by He et al. (2002, 2003) to measure directly the temperature decays along the femoral arteries and veins and their subsequent branches in rats. The experimental results have demonstrated that the venous blood in mid-size blood veins recaptured up to 41 percent of the total heat released from their countercurrent arteries under normal conditions. As expected, the contribution of countercurrent rewarming is reduced significantly to less than 15 percent for hyperemic conditions.

In a series of experiments with an isolated perfused bovine kidney, Crezee and Lagendijk (1990) inserted a small plastic tube into the tissue of a bovine kidney and measured the resulting temperature fields in a plane perpendicular to the tube while heated water was circulated through it, with the kidney cortex perfused at different rates. They also used thermocouples to map the temperature distribution in the tissue of isolated bovine tongues perfused at various perfusion rates (Crezee et al., 1991). By examining the effect of increased perfusion on the amplitude and width of the thermal profile, they demonstrated that the temperature measurements agreed better with a perfusion-enhanced k_{eff} as opposed to the perfusion source term in the Pennes equation.

Charny (Charny et al., 1990) developed a detailed one-dimensional three-equation model. Since this model was based on energy conservation and no other assumptions were introduced to simplify the analysis of the blood flow effect, it was viewed as a relatively more accurate model than both the Pennes and Weinbaum-Jiji equation. The validity of the assumptions inherent in the formulation of the Weinbaum-Jiji equation was tested numerically under different physiological conditions. In addition, the temperature profile predicted by the Pennes model was compared with that by the three-equation model and the difference between them was evaluated. The numerical simulation of the

axial temperature distribution in the limb showed that the Weinbaum-Jiji bioheat equation provided very good agreement with the three-equation model for downstream vascular generations that are located in the outer layer in the limb muscle, while the Pennes model yielded better description of heat transfer in the upstream vessel generations. Considering that vessels bifurcate from approximately 1000 μm in the first generation to 150 μm in the last generation, one finds that the Pennes source term, which was originally intended to represent an isotropic heat source in the capillaries, is shown to describe instead the heat transfer from the largest countercurrent vessels, more than 500 μm in diameter. The authors concluded that this was largely attributed to the capillary bleed-off from the large vessels in these tissue regions. The capillary bleed-off appeared to result in a heat source type of behavior that matches the Pennes perfusion term. The Weinbaum-Jiji model, on the other hand significantly overestimated the countercurrent heat exchange in the tissue region containing larger blood vessels. The validity of the Weinbaum-Jiji equation requires that the ratio of the thermal equilibration length L_e of the blood vessel to its physical length L be less than 0.2. This criterion was found to be satisfied for blood vessels less than 300 μm in diameter under normothermic conditions.

2.3.3 Heat Transfer Models of the Whole Body

As outlined above, due to the complexity of the vasculature, continuum models appear more favorable in simulating the temperature field of the human body. In the Pennes bioheat equation, blood temperature is considered to be the same as the body core temperature; in the Weinbaum-Jiji bioheat equation, on the other hand, the effect of the blood temperature serves as the boundary condition of the simulated tissue domain. In either continuum model (Pennes or Weinbaum-Jiji), blood temperature is an input to the governing equation of the tissue temperature. However, in situations in which the blood temperature is actively lowered or elevated, both continuum models seem inadequate to account for the tissue-blood thermal interactions and to accurately predict the expected body temperature changes.

The human body has limited ability to maintain a normal, or euthermic, body temperature. The vasculature facilitates the redistribution and transfer of heat throughout the body preserving a steady core temperature for all vital organs and making the human body relatively insensitive to environmental temperature changes. In extreme situation such as heavy exercise or harsh thermal environment, the body temperature can shift to a high or low level from the normal range. Active control of body temperature is increasingly employed therapeutically in several clinical scenarios, most commonly to protect the brain from the consequences of either primary (i.e., head trauma, stroke) or secondary injury (i.e., after cardiac arrest with brain hypoperfusion). Mild to moderate hypothermia, during which brain temperature is reduced to 30 to 35°C, has been studied, among others, as an adjunct treatment for protection from cerebral ischemia during cardiac bypass injury (Nussmeier, 2002), carotid endarterectomy (Jamieson et al., 2003), and resection of aneurysms (Wagner and Zuccarello, 2005), and it is also commonly employed in massive stroke and traumatic brain injury patients (Marion et al., 1996, 1997). Even mild reductions in brain temperature as small as 1°C and importantly, the avoidance of any hyperthermia, can substantially reduce ischemic cell damage (Clark et al., 1996; Wass et al., 1995) and improve outcome (Reith et al., 1996). It seems that either the Pennes or Weinbaum-Jiji bioheat equation alone is unable to predict how the body/blood temperature changes during those situations.

Understanding the blood temperature variation requires a theoretical model to evaluate the overall blood-tissue thermal interaction in the whole body. The theoretical models developed by Wissler and other investigators (Fu, 1995; Salloum, 2005; Smith, 1991; Wissler, 1985) similarly introduced the whole body as a combination of multiple compartments. The majority of the previously published studies introduced a pair of countercurrent artery and vein with their respective branching (flow system) in each compartment and then modeled the temperature variations along this flow system to derive the heat transfer between the blood vessels and tissue within each flow segment. The accuracy of those approaches of applying a countercurrent vessel pair and their subsequent branches has not been verified by experimental data. Such an approach is also computationally intensive, although the models are capable of delineating the temperature decay along the artery and the rewarming by the countercurrent vein.

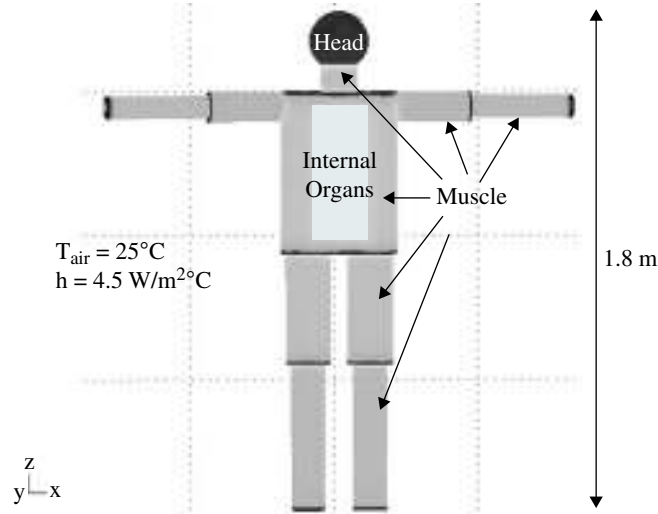


FIGURE 2.3 Schematic diagram of the whole body geometry.

A recently developed whole body model by our group (Zhu et al., 2009) utilizes the simple representation of the Pennes perfusion source term to assess the overall thermal interaction between the tissue and blood in the human body. As shown in Fig. 2.3, a typical human body (male) has a body weight of 81 kg and a volume of 0.074 m³. The body consists of limbs, torso (internal organs and muscle), neck, and head. The limbs and neck are modeled as cylinders consisting of muscle. Note that the body geometry can be modeled more realistically if one includes a skin layer and a fat layer in each compartment. However, since our objective is to illustrate the principle and feasibility of the developed model, those details are neglected in the sample calculation. The simple geometry results in a body surface area of 1.8 m². Applying the Pennes bioheat equation to the whole body yields

$$\rho_t c_t \frac{\partial T_t}{\partial t} = k_t \nabla^2 T_t + q_m + \rho_b c_b \omega (T_a - T_t) \quad (2.8)$$

where subscripts t and b refer to tissue and blood, respectively; T_t and T_a are body tissue temperature and blood temperature, respectively; ρ is density; c is specific heat; k_t is thermal conductivity of tissue; q_m is the volumetric heat generation rate (W/m³) due to metabolism; and ω is the local blood perfusion rate. The above governing equation can be solved once the boundary conditions and initial condition are prescribed. The boundary at the skin surface is modeled as a convection boundary subject to an environment temperature of T_{air} and a convection coefficient of h .

Based on the Pennes bioheat equation, the rate of the total heat loss from the blood to tissue at any time instant is

$$Q_{\text{blood-tissue}} = \iiint_{\text{body volume}} \rho_b c_b \omega (T_a(t) - T_t) dV_{\text{body}} = \rho_b c_b \bar{\omega} (T_a(t) - \bar{T}_t) V_{\text{body}} \quad (2.9)$$

where V_{body} is the body volume, T_a is the blood temperature which may vary with time. Equation (2.9) implies that both density ρ and specific heat c are constant. In Eq. (2.9), $\bar{\omega}$ is the volumetric average blood perfusion rate defined as

$$\bar{\omega} = \frac{1}{V_{\text{body}}} \iiint_{\text{body volume}} \omega dV_{\text{body}} \quad (2.10)$$

\bar{T}_t is the weighted average tissue temperature defined by Eq. (2.9) and is given by

$$\rho c \bar{\omega} (T_{a0} - \bar{T}_t) V_{\text{body}} = \iiint_{\text{body volume}} \rho c \omega (T_a - T_t) dV_{\text{body}} \quad (2.11)$$

where in Eq. (2.11), T_t can be determined by solving the Pennes bioheat equation.

During clinical applications, external heating or cooling of the blood can be implemented to manipulate the body temperature. In the study of Zhu et al. (2009), the blood in the human body is represented as a lumped system. It is assumed that a typical value of the blood volume of body, V_b , is approximately 5 L. External heating or cooling approaches can be implemented via an intravascular catheter or intravenous fluid infusion. A mathematical expression of the energy absorbed or removed per unit time is determined by the temperature change of the blood, and is written as

$$\rho_b c_b V_b [T_a(t + \Delta t) - T_a(t)] / \Delta t \approx \rho_b c_b V_b \frac{dT_a}{dt} \quad (2.12)$$

where $T_a(t)$ is the blood temperature at time, t , and $T_a(t + \Delta t)$ is at time $t + \Delta t$. In the mathematical model, we propose that energy change in blood is due to the energy added or removed by external heating or cooling (Q_{ext}), and heat loss to the body tissue in the systemic circulation ($Q_{\text{blood-tissue}}$). Therefore, the governing equation for the blood temperature can be written as

$$\rho_b c_b V_b \frac{dT_a}{dt} = Q_{\text{ext}}(T_a, t) - Q_{\text{blood-tissue}}(t) = Q_{\text{ext}}(T_a, t) - \rho_b c_b \bar{\omega} V_{\text{body}} (T_a - \bar{T}_t) \quad (2.13)$$

where Q_{ext} can be a function of time and the blood temperature due to thermal interaction between blood and the external cooling approach, T_a , \bar{T}_t , and $\bar{\omega}$ can be a function of time. Equation (2.13) cannot be solved alone since \bar{T}_t is determined by solving the Pennes bioheat equation. One needs to solve Eqs. (2.8) and (2.13) simultaneously.

One application of blood cooling involves pumping coolant into the inner tube of a catheter inserted into the femoral vein and advanced to the veno-vena. Once the coolant reaches the catheter, it flows back from the outer layer of the catheter and out of the cooling device. This cooling device has been used in clinical trials in recent years as an effective approach to decrease the temperature of the body for stroke or head injury patients. Based on previous research of this device, the cooling capacity of the device is around -100 W [Q_{ext} in Eq. (2.13)].

Figure 2.4 gives the maximum tissue temperature, the minimum tissue temperature at the skin surface, the volumetric-average body temperature (T_{avg}), and the weighted-average body temperature (\bar{T}_t). The difference between the volumetric-average body temperature and the weighted-average-body temperature is due to their different definitions. All tissue temperatures decrease almost linearly with time and after 20 minutes, the cooling results in approximately 0.3 to 0.5°C tissue temperature drop. The cooling rate of the skin temperature is smaller ($0.2^\circ\text{C}/20$ min). As shown in Fig. 2.5, the initial cooling rate of the blood temperature in the detailed model is very high ($\sim 0.14^\circ\text{C}/\text{min}$), and then it decreases gradually until it is stabilized after approximately 20 minutes. On the other hand, cooling the entire body (the volumetric average body temperature) starts slowly and gradually catches up. It may be due to the inertia of the body mass in responding to the cooling of the blood. Figure 2.5 also illustrates that after the initial cooling rate variation, the stabilized cooling rates of all temperatures approach each other and they are approximately $0.019^\circ\text{C}/\text{min}$ or $1.15^\circ\text{C}/\text{h}$. The simulated results demonstrate the feasibility of inducing mild body hypothermia (34°C) within 3 hours using the cooling approach.

The developed model in Zhu et al. (2009) using the Pennes perfusion term and lumped system of the blood is simple to use in comparison with these previous whole body models while providing meaningful and accurate theoretical estimates. It also requires less computational resources and time. Although the model was developed for applications involving blood cooling or rewarming, the detailed geometry can also be used to accurately predict the body temperature changes during exercise.

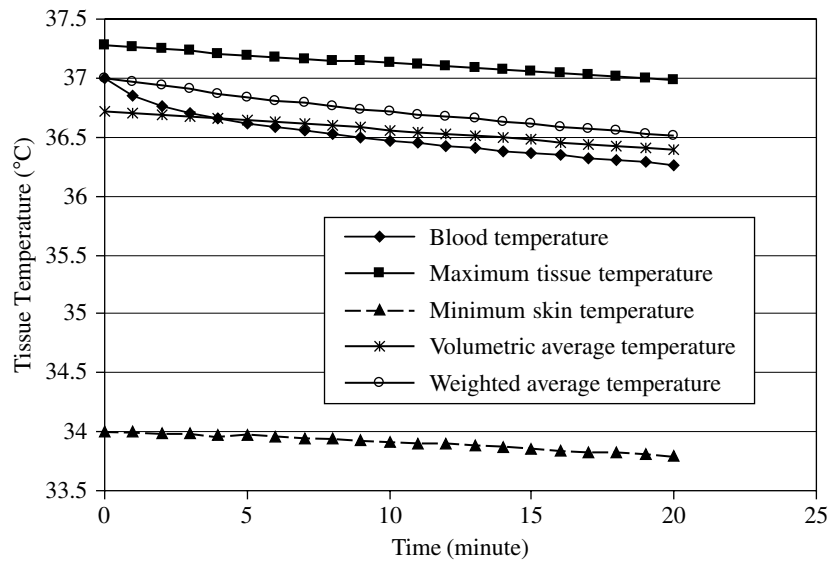


FIGURE 2.4 Temperature decays during the cooling process using the implicit scheme.

It is well known that strenuous exercise increases cardiac output, redistributes blood flow from internal organs to muscle, increases metabolism in exercising muscle, and enhances heat transfer to the skin. The whole body model can be easily modified to also include a skin layer and a fat layer in the compartments of the limbs. Further, redistribution of blood flow from the internal organs to the musculature can be modeled as changes of the local blood perfusion rate in the respective compartments and the enhanced skin heat transfer can be adjusted for by inducing evaporation at the skin surface

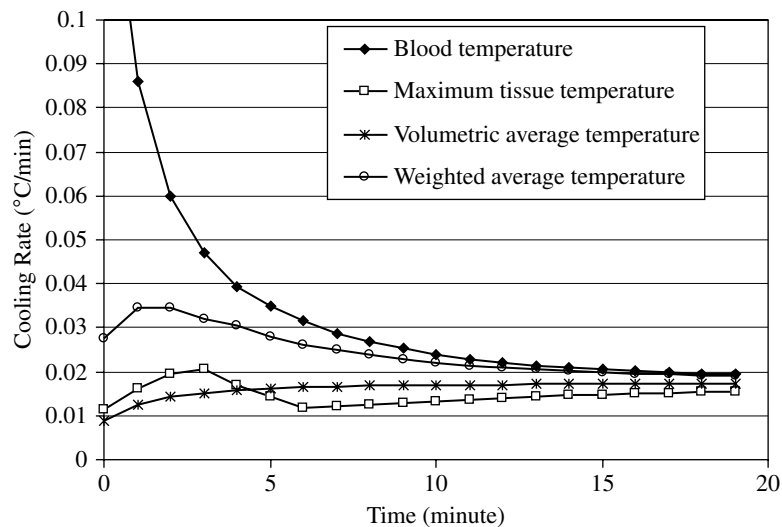


FIGURE 2.5 Induced cooling rates of the blood temperature, the maximum temperature, the volumetric average temperature, and the weighted average temperature.

and/or taking off clothes to increase the overall heat transfer coefficient h . Therefore, one can use the model to accurately delineate important clinical scenarios such as heat stroke, and predict body temperature elevations during heavy exercise and/or heat exposures.

2.4 TEMPERATURE, THERMAL PROPERTY, AND BLOOD FLOW MEASUREMENTS

2.4.1 Temperature

The control of human body temperature is a complex mechanism involving release of neurotransmitters and hormones, redistributing blood flow to the skin, respiration, evaporation, and adjusting metabolic rate. The control mechanism can be altered by certain pathologic (fever) and external (hyperthermia treatment) events. Consequently, temperature is an important parameter in the diagnosis and treatment for many diseases. Elevated local tissue temperature can be an indication of excess or abnormal metabolic rates. Inflammation is the body's response to attacks and a mechanism for removing foreign or diseased substances. Exercise also induces an increase in local temperature of skeletal muscles and joints. Some diagnostic procedures involve the measurement of temperatures. Thermal images of the breast surface have been used to detect the presence of malignant tumors. Temperature measurement is also critical in many therapeutic procedures involved in either hyperthermia or hypothermia.

Temperature-measuring devices can fall into two categories, invasive and noninvasive. Invasive temperature sensors offer the advantages of small size, fast response time, extreme sensitivity to temperature changes, and high stability. However, they have generally involved a limited number of measurement locations, uncertainties about the anatomic placement of thermometry devices, interaction with the energy field applied, periodic rather than continuous temperature monitoring, and, in some cases, surgical exposure of the target tissue for placement of the temperature probes.

Invasive temperature devices include thermocouples, thermistor beads, optical fiber sensors, etc. A thermocouple consists of two pieces of dissimilar metal that form two junctions. In the wire, an electric potential difference is formed if there exists a temperature difference between the two junctions. This potential difference can be measured with a high resolution voltmeter and translated to temperature with a fairly simple means of calibration. A thermocouple usually has a good long-term stability, responds very quickly to changes in temperature due to its small thermal capacity, and can be constructed in a manner that allows a good resolution. Another kind of invasive device, the thermistor bead, is made by depositing a small quantity of semiconductor paste onto closely spaced metal wires. The wire and beads are sintered at a high temperature when the material forms a tight bond. The wires are then coated with glass or epoxy for protection and stabilization. The resistors generally exhibit high thermal sensitivity. This characteristic sensitivity to temperature change can result in a change of thermistor resistance of more than $50 \Omega/^{\circ}\text{C}$. Unlike a thermocouple or a thermistor bead, the fiber optic temperature probe does not interfere with an electromagnetic field. It has been used to measure tissue temperature rise induced by microwave and/or radio frequency heating (Zhu et al., 1996b, 1998). However, it is relatively big in size (~ 1.5 mm in diameter) and has a lower temperature resolution ($\sim 0.2^{\circ}\text{C}$).

Noninvasive temperature-measuring techniques include MRI thermometry, infrared thermography, etc. Because of the theoretical sensitivity of some of its parameters to temperature, MRI has been considered to be a potential noninvasive method of mapping temperature changes during therapies using various forms of hyperthermia. MRI imaging has the advantage of producing three-dimensional anatomic images of any part of the body in any orientation. In clinical practice, MRI characteristic parameters such as the molecular diffusion coefficient of water, the proton spin-lattice (T_1) relaxation time (Parker et al., 1982), and the temperature-dependent proton resonance frequency (PRF) shift have been used to estimate the in vivo temperature distribution in tissues. MRI provides good spatial localization and sufficient temperature sensitivity. At the present time, it also appears to be the most promising modality to conduct basic assessments of heating systems and

techniques. The disadvantages of MRI thermometry include limited temporal resolution (i.e., quasi-real time), high environmental sensitivity, high material expenditure, and high running costs.

Infrared thermography is based on Planck's distribution law describing the relationship between the emissive power and the temperature of a blackbody surface. The total radiative energy emitted by an object can be found by integrating the Planck equation for all wavelengths. This integration gives the Stefan-Boltzmann law $E(T) = \epsilon\sigma T^4$. The thermal spectrum as observed by an infrared-sensitive detector can be formed primarily by the emitted light. Hence, the formed thermal image is determined by the local surface temperature and the emissivity of the surface. If the emissivity of the object is known, and no intervening attenuating medium exists, the surface temperature can be quantified. Quantification of skin temperature is possible because the human skin is almost a perfect blackbody ($\epsilon = 0.98$) over the wavelengths of interest. A recent numerical simulation of the temperature field of breast (Hu et al., 2004) suggests that image subtraction could be employed to improve the thermal signature of the tumor on the skin surface. Drug-induced vascular constriction in the breast can further enhance the ability of infrared thermography in detecting deep-seated tumor. Qualitative thermography has been successfully used in a wide range of medical applications (Jones, 1998) including cardiovascular surgery (Fiorini et al., 1982), breast cancer diagnoses (Gautherie and Gros, 1980; Lapayowker and Revesz, 1980), tumor hyperthermia (Cetas et al., 1980), laser angioplasty, and peripheral venous disease. Clinical studies on patients who had breast thermography demonstrated that an abnormal thermography was associated with an increased risk of breast cancer and a poorer prognosis for the breast cancer patients (Gautherie and Gros, 1980; Head et al., 1993). Infrared tympanic thermometry has also been developed and widely used in clinical practice and thermoregulatory research as a simple and rapid device to estimate the body core temperature (Matsukawa et al., 1996; Shibasaki et al., 1998).

2.4.2 Thermal Property (Thermal Conductivity and Thermal Diffusivity) Measurements

Knowledge of thermal properties of biological tissues is fundamental to understanding heat transfer processes in the biological system. This knowledge has increased importance in view of the concerns for radiological safety with microwave and ultrasound irradiation, and with the renewed interest in local and regional hyperthermia as a cancer therapy. The availability of a technique capable of accurately characterizing thermal properties of both diseased and normal tissue would greatly improve the predictive ability of theoretical modeling and lead to better diagnostic and therapeutic tools.

The primary requirement in designing an apparatus to measure thermal conductivity and diffusivity is that the total energy supplied should be used to establish the observed temperature distribution within the specimen. For accurate measurements, a number of structural and environmental factors, such as undesired heat conduction to or from the specimen, convection currents caused by temperature-induced density variations, and thermal radiation, must be minimized. Biomaterials present additional difficulties. The existing literature on biological heat transfer bears convincing evidence of the complexity of heat transfer processes in living tissue. For example, thermal properties of living tissue differ from those of excised tissue. Clearly the presence of blood perfusion is a major factor in this difference. Relatively large differences in thermal conductivity exist between similar tissues and organs, and variations for the same organ, are frequently reported. Such variations suggest the importance of both defining the measurement conditions and establishing a reliable measurement technique.

The thermal property measurement techniques can be categorized as steady-state methods and transient methods. They can also be categorized as invasive and noninvasive techniques. In general, determining thermal properties of tissue is conducted by an inverse heat transfer analysis during which either the temperatures or heat transfer rates are measured in a well-designed experimental setup. The major challenge is to design the experiment so that a theoretical analysis of the temperature field of the experimental specimen can be as simple as possible to determine the thermal property from the measured temperatures. It is usually preferred that an analytical solution of the temperature field can be derived. In the following sections, those principles are illustrated by several widely used techniques for measuring tissue thermal conductivity or diffusivity. Their advantages and limitations will also be described.

Guarded Hot Plate. Thermal conductivity can be measured directly by using steady-state methods, such as the guarded hot plate. This method is invasive in that it requires the excision of the specimen for in vitro measurement. It typically involves imposing a constant heat flux through a specimen and measuring the temperature profile at specific points in the specimen after a steady-state temperature field has been established. Once a simple one-dimensional steady-state temperature field is established in the specimen, the thermal conductivity may be easily found by the expression based on the linear temperature profile in a one-dimensional wall

$$k = \frac{q''L}{T_1 - T_2} \quad (2.14)$$

where q'' is the heat flux passing through the specimen, T_1 and T_2 are temperature values at any two measurement locations in the axial direction (or the direction of the heat flux), and L is the axial distance between these two temperature measurements.

Biological materials typically have moderate thermal conductivities and therefore, require extensive insulation to ensure a unidirectional heat flow in the one-dimensional wall. The contact resistance between the specimen and the plate is also difficult to be minimized. In addition, this method cannot be used to obtain in vivo measurements. Once the tissue specimen is cut from the body, dehydration and temperature-dependent properties may need to be considered. It is also a challenge to accurately measure the thickness of the tissue sample.

Flash Method. The transient flash method, first proposed by Parker et al. (1961), is the current standard for measuring the thermal diffusivity of solids. A schematic diagram of this method is shown in Fig. 2.6. The front face of a thin opaque solid, of uniform thickness, is exposed to a burst of intense radiant energy by either a high-energy flash tube or laser. The method assumes that the burst of energy is absorbed instantaneously by a thin layer at the surface of the specimen. Adiabatic boundary conditions are assumed on all other surfaces and on the front face during the measurement. The transient temperature at the rear surface is then measured by using thermocouples or an infrared detector.

An analytic expression for the rear surface temperature transient in the one-dimensional temperature field is given by

$$T(l,t) - T(l,0) = \frac{Q}{\rho Cl} \left[1 + 2 \sum_{n=1}^{\infty} (-1)^n \exp\left(-\frac{n^2 \pi^2}{l^2} \alpha t\right) \right] \quad (2.15)$$

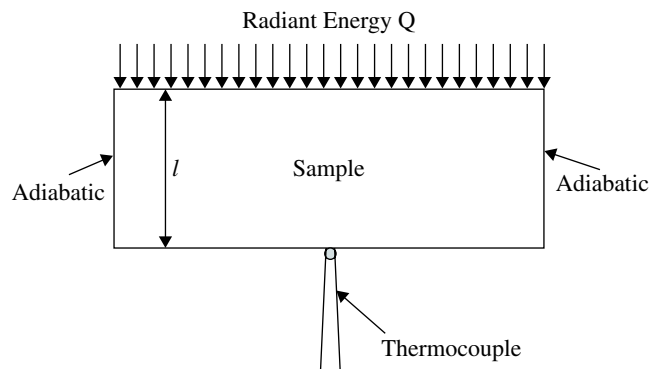


FIGURE 2.6 Schematic diagram of a flash apparatus for sample diffusivity measurements.

where Q = absorbed radiant energy per unit area

ρ = mass density

C = specific heat

l = sample thickness

α = thermal diffusivity

The maximum temperature at the rear surface is determined by the volumetric heating as

$$T_{\max} = T(l, 0) + Q/(\rho C l) \quad (2.16)$$

The thermal diffusivity in the direction of heat flow is usually calculated by the expression

$$\alpha = 1.38 \frac{l^2}{\pi^2 t_{1/2}} \quad (2.17)$$

where $t_{1/2}$ is the time required for the rear surface to reach half of its maximum temperature.

The simplicity of the method described above is often offset by the difficulty in satisfying the required adiabatic boundary conditions. In order for this solution to be valid, the radiant energy incident on the front surface is required to be uniform, and the duration of the flash must be sufficiently short compared with the thermal characteristic time of the sample. In addition, it assumes that the sample is homogeneous, isotropic, and opaque, and that the thermal properties of the sample do not vary considerably with temperature.

Temperature Pulse Decay (TPD) Technique. Temperature pulse decay (TPD) technique is based on the approach described and developed by Arkin, Chen, and Holmes (Arkin et al., 1986, 1987). This method needs no insulation, in contrast to some of the methods described above, since testing times are short, usually on the order of seconds. However, the determination of the thermal conductivity or the blood flow rate requires the solution of the transient bioheat transfer equation.

This technique employs a single thermistor serving as both a temperature sensor and a heater. Typically in this technique, either a thermistor is inserted through the lumen of a hypodermic needle, which is in turn inserted into the tissue, or the thermistor is embedded in a glass-fiber-reinforced epoxy shaft. Figure 2.7 shows the structure of a thermistor bead probe embedded in an epoxy shaft. Each probe can consist of one or two small thermistor beads situated at the end or near the middle of the epoxy shaft. The diameter of the finished probe is typically 0.3 mm, and the length can vary as desired. Because the end can be sharpened to a point, it is capable of piercing most tissues with very minimal trauma.

During the experiment, a short-heating pulse of approximately 3 seconds is delivered by the thermistor bead. The pulse heating results in a temperature rise in the area near the tip of the probe. After the pulse heating, the temperature of the probe will decrease. During the pulse heating and its subsequent temperature decay, the temperature at the tip of the probe is measured by the thermistor bead. To determine the thermal conductivity or blood flow rate, a theoretical prediction of the transient temperature profile is needed for the same tissue domain as in the experimental study. Typically, the theoretically predicted temperature profile is obtained by solving a bioheat transfer equation in which the blood flow rate and thermal conductivity have to be given as input to the model. The predicted temperature profile is then compared with the experimental measurements. The values of the blood flow rate and/or thermal conductivity will be adjusted to minimize the square difference between the predicted temperature profile and the experimental measurements using the linear-square residual fit. The values for the blood flow rate and thermal conductivity that give the best fit of the experimentally measured temperature profile are the calculated blood flow rate and thermal conductivity of the tissue sample.

Typically, the Pennes bioheat transfer equation is used to predict the temperature transient. It is assumed that the thermistor bead is small enough to be considered a point source inserted into the center of an infinitely large medium. The governing equation and initial condition for this thermal

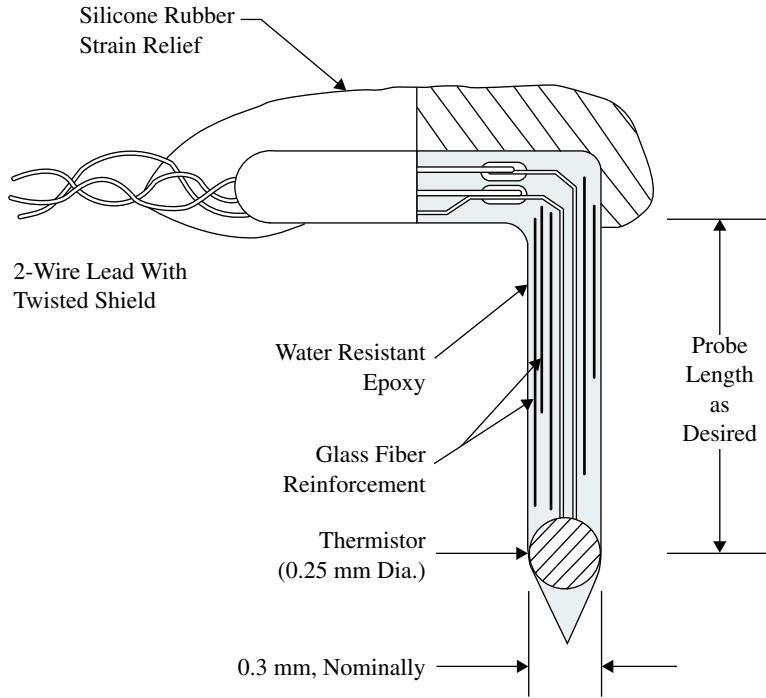


FIGURE 2.7 Sketch of a thermistor bead probe. [From Xu et al. (1998), with permission.]

process are described as

$$\rho C \frac{\partial T_t}{\partial t} = k_t \frac{1}{r} \frac{\partial}{\partial r} \left(r \frac{\partial T_t}{\partial r} \right) + \omega \rho C (T_a - T_t) + q_p \quad (2.18)$$

$$t = 0 \quad T_t = T_{ss}(r)$$

where q_p is the pulse heating deposited locally into the tissue through a very small thermistor bead probe as $q_p = P \delta(0)$ for $t \leq t_p$; $q_p = 0$ for $t > t_p$. P is the deposited power, and $\delta(0)$ is the Dirac delta function. Before the measurement, the steady-state temperature distribution $T_{ss}(r)$ in the sample should satisfy the one-dimensional steady-state conduction equation without the pulse heating. The governing equation for $T_{ss}(r)$ is given by

$$0 = k_t \frac{1}{r} \frac{d}{dr} \left(r \frac{dT_{ss}}{dr} \right) + \omega \rho C (T_a - T_{ss}) \quad (2.19)$$

Subtracting Eq. (2.19) from Eq. (2.18), and introducing $\theta = T_t - T_{ss}$, one obtains

$$\rho C \frac{\partial \theta}{\partial t} = k_t \frac{1}{r} \frac{\partial}{\partial r} \left(r \frac{\partial \theta}{\partial r} \right) + \omega \rho C \theta + q_p \quad (2.20)$$

$$t = 0 \quad \theta = 0$$

For the limiting case of an infinitesimally small probe with an infinitesimally short heating pulse, the solution for Eq. (2.20) for the interval of temperature decay takes the form

$$\theta = \lambda_2 \int_0^{t_0} (t-s)^{-1.5} e^{-\omega(t-s)} e^{-r^2/[4\lambda_1(t-s)]} ds \quad (2.21)$$

where $\lambda_1 = P(\rho C)^{0.5}/(8\pi^{1.5})$ and $\lambda_2 = \alpha/(k_t^{1.5} t_p^{0.5})$. In this theoretical analysis, there are two unknowns, k_t and α . A least square residual fit allows one to find a set of values of k_t and ω that will lead to the best fit of the theoretical predictions to the experimentally measured temperature decay.

The temperature pulse decay technique has been used to measure both the in vivo and in vitro thermal conductivity and blood flow rate in various tissues (Xu et al., 1991, 1998). The specimen does not need to be cut from the body, and this method minimizes the trauma by sensing the temperature with a very small thermistor bead. For the in vitro experimental measurement, the measurement of thermal conductivity is simple and relatively accurate. The infinitively large tissue area surrounding the probe implies that the area affected by the pulse heating is very small in comparison with the tissue region. This technique also requires that the temperature distribution before the pulse heating should reach steady state in the surrounding area of the probe.

2.4.3 Blood Perfusion Measurement

Blood perfusion rate is defined as the amount of blood supplied to a certain tissue region per minute per 100 g tissue weight. In most of the situation, it is representing the nutrient need in that tissue area. High blood perfusion is also associated with heat dissipation during exercise or thermal stress. In humans, there are several tissue regions, such as kidney, heart, and choriocapillaris in the eye, possessing a high blood perfusion rate. The measured blood perfusion rate in the kidney is approximately 500 mL/min/100 g tissue (Holmes, 1997). In the heart, the blood perfusion rate is around 300 mL/min/100 g which serves for the energy need of pumping the heart. The choriocapillaris in the eyes is a meshed structure within two thin sheets. Its blood perfusion rate is very high and can be as much as 8000 mL/min/100 g tissue. In addition to providing oxygen and other nutrients to the retina, the choriocapillaris also may play a role in stabilizing the temperature environment of the retina and retinal pigment epithelium (Aurer and Carpenter, 1980). In addition to its physiological role, blood perfusion measurement is important in theoretical modeling of the temperature distribution during various therapeutic and diagnostic applications.

Radio-Labeled Microsphere Technique. Measurement of blood flow has become an integral part of the physiologic study of humans. While many methods have been utilized in measuring tissue blood flow, the one most often practiced today is dependent on injection of radioactively labeled microspheres. The reason for its overwhelming acceptance is due, in part, to the shortcomings of many of the alternative methods of blood flow determination.

In principle, small particles are uniformly mixed with blood and allowed to circulate freely until they impact in a vessel smaller in diameter than themselves. The tissue or organ is then removed and its radioactivity measured. In such a system, the number of particles impacted in a given tissue is assumed proportional to the volume of particle-containing blood perfusing that tissue. If the number of particles in the tissue sample is determined, and an adequate blood flow reference established, a tissue blood flow can be derived.

Calculating the blood flow rate is straightforward; it is based on the assumption that the number of microspheres in each organ should be directly proportional to blood flow to that organ, e.g.,

$$\frac{\text{Blood flow to organ A}}{\text{Microspheres in organ A}} = \frac{\text{blood flow to organ B}}{\text{microspheres in organ B}} = \frac{\text{cardiac output}}{\text{total microspheres injected}} \quad (2.22)$$

The cardiac output of the animal is obtained by another independent method.

Like any other experimental method, determination of blood flow by radioactive microspheres is subject to many sources of error, including individual variation among the sample population, the counting accuracy of the total microspheres in the tissue sample by the gamma counter, and the effect of arteriovenous shunting or the migration of the microspheres. Despite all the limitations of this method, the microsphere technique of blood flow determination has become the most powerful method available today and has been used to evaluate the accuracy of other techniques of blood flow measurement.

Doppler Ultrasound. Doppler ultrasound has been widely used to provide qualitative measurements of the average flow velocity in large to medium-size vessels if the vessel diameter is known. These include the extracranial circulation and peripheral limb vessels. It is also used in an assessment of mapped occlusive disease of the lower extremities. The frequency used for Doppler ultrasound is typically between 1 and 15 MHz. The basis of this method is the Doppler shift, which is the observed difference in frequency between sound waves that are transmitted from simple piezoelectric transducers and those that are received back when both transmitter and receiver are in relative motion. The average frequency shift of the Doppler spectrum is proportional to the average particulate velocity over the cross-sectional area of the sample. When used to measure blood flow, the transducers are stationary and motion is imparted by the flowing blood cells. In this event, red cell velocity V is described by the relationship

$$\delta F/F = (2V/C) \cos\theta \quad \text{or} \quad V = \delta F/F (C/2\cos) \quad (2.23)$$

where δF = frequency change of the emitted wave

C = mean propagation velocity of ultrasound within tissues (about 1540 m/s)

θ = angle between the ultrasound beam and the flow velocity

The frequency shift is usually in the audible range and can be detected by an audible pitch variation or can be plotted graphically.

Attenuation of ultrasound increases nearly linearly with frequency in many types of tissue, causing high frequencies to be attenuated more strongly than low frequencies. The depth of penetration of the signal also depends on the density of the fluid; hence sampling of the velocity profile could be inaccurate in situations where this can vary. Determination of absolute flow/tissue mass with this technique has limited potential, since vessel diameter is not accurately measured and volume flow is not recorded. It is not possible, using currently available systems, to accurately measure the angle made by the ultrasonic beam and the velocity vector. Thus, Doppler flow measurements are semiquantitative.

Laser Doppler Flowmetry. Laser Doppler flowmetry (LDF) offers the potential to measure flow in small regional volumes continuously and with repetitive accuracy. It is ideally suited to measure surface flow on skin or mucosa or following surgical exposure. LDF couples the Doppler principle in detecting the frequency shift of laser light imparted by moving red blood vessels in the blood stream. Incident light is carried to the tissue by fiber optic cables, where it is scattered by the moving red blood cells. By sampling all reflected light, the device can calculate flux of red blood cells within the sample volume. Depending on the light frequency, laser light penetrates tissue to a depth of less than approximately 3 mm.

The output from LDF is measured not in easily interpretable units of flow but rather in hertz. It would be ideal to define a single calibration factor that could be used in all tissues to convert laser output to flow in absolute units. Unfortunately, the calibration to determine an absolute flow is limited by the lack of a comparable standard and the lack of preset controlled conditions. This may be due to varying tissue optical properties affected by tissue density (Obeid et al., 1990). Further, LDF signals can be affected by movement of the probe relative to the tissue.

Despite its limitations, LDF continues to find widespread applications in areas of clinical research because of its small probe size, high spatial and temporal resolution, and entire lack of tissue contact if required. It has been suggested that LDF is well suited for comparisons of relative changes in blood flow during different experimental conditions (Smits et al., 1986). It is especially valuable to provide a direct measurement of cutaneous blood flow. In patients with Raynaud's

phenomenon, it has been indicated that the abnormal cutaneous blood flow is related to the diminished fibrinolytic activity and increased blood viscosity (Engelhart and Kristensen, 1986). LDF has also been useful for assessing patients with fixed arterial obstructive disease of the lower extremity (Schabauer and Rooke, 1994). Other cutaneous uses of LDF include postoperative monitoring of digit reattachment, free tissue flap, and facial operations (Schabauer and Rooke, 1994). In the noncutaneous application of LDF, it has been reported to measure the retinal blood flow in patients with diabetes mellitus. LDF has also been used to monitor cerebral blood perfusion (Borgos, 1996). Recently, it was used to evaluate the brain autoregulation in patients with head injury (Lam et al., 1997).

Temperature Pulse Decay Technique. As described in subsection “Temperature Pulse Decay (TPD) technique,” local blood perfusion rate can be derived from the comparison between the theoretically predicted and experimentally measured temperature decay of a thermistor bead probe. The details of the measurement mechanism have been described in that section. The temperature pulse decay technique has been used to measure the *in vivo* blood perfusion rates of different physical or physiological conditions in various tissues (Xu et al., 1991, 1998; Zhu et al., 2005). The advantages of this technique are that it is fast and induces little trauma. Using the Pennes bioheat transfer equation, the intrinsic thermal conductivity and blood perfusion rate can be simultaneously measured. In some of the applications, a two-parameter least-square residual fit was first performed to obtain the intrinsic thermal conductivity of the tissue. This calculated value of thermal conductivity was then used to perform a one-parameter curve fit for the TPD measurements to obtain the local blood perfusion rate at the probe location. The error of blood perfusion measurement using the TPD technique is mainly inherited from the accuracy of the bioheat transfer equation. Theoretical study (Xu et al., 1993) has shown that this measurement is affected by the presence of large blood vessels in the vicinity of the thermistor bead probe. Further, poor curve fitting of the blood perfusion rate occurs if the steady state of the tissue temperature is not established before the heating (Xu et al., 1998).

2.5 HYPERTHERMIA TREATMENT FOR CANCERS AND TUMORS

2.5.1 Introduction

Within the past two decades, there have been important advances in the use of hyperthermia in a wide variety of therapeutic procedures, especially for cancer treatment. Hyperthermia is used either as a singular therapy or as an adjuvant therapy with radiation and drugs in human malignancy. It has fewer complications and is preferable to more costly and risky surgical treatment (Dewhirst et al., 1997). The treatment objective of current therapy is to raise tumor temperature higher than 43°C for periods of more than 30 to 60 minutes while keeping temperatures in the surrounding normal tissue below 43°C. It has been suggested that such elevated temperatures may produce a heat-induced cytotoxic response and/or increase the cytotoxic effects of radiation and drugs. Both the direct cell-killing effects of heat and the sensitization of other agents by heat are phenomena strongly dependent on the achieved temperature rise and the heating duration.

One of the problems encountered by physicians is that current hyperthermia technology cannot deliver adequate power to result in effective tumor heating of all sites. The necessity of developing a reliable and accurate predictive ability for planning hyperthermia protocols is obvious. The treatment planning typically requires the determination of the energy absorption distribution in the tumor and normal tissue and the resulting temperature distributions. The heating patterns induced by various hyperthermia apparatus have to be studied to focus the energy on a given region of the body and provide a means for protecting the surrounding normal tissues. Over the past two decades, optimization of the thermal dose is possible with known spatial and temporal temperature distribution during the hyperthermia treatment. However, large spatial and temporal variations in temperature are still observed because of the heterogeneity of tissue properties (both normal tissue and tumor), spatial variations in specific absorption rates, and the variations and dynamics of blood flow (Overgaard, 1987). It has been suggested that blood flow in large, thermally unequilibrated vessels is the main cause for temperature nonhomogeneity during hyperthermia treatment, since these large vessels can

produce cold tracts in the heated volume. Thus, to heat the tissue and tumor volume effectively and safely, it is critical to experimentally or theoretically monitor the temporal and spatial temperature gradient during the hyperthermia treatment.

2.5.2 Temperature Monitoring during Thermal Treatment

One of the reasons hyperthermia has not yet become widely accepted as a mode of therapy is the lack of noninvasive and inexpensive temperature measurement technology for routine use. Invasive temperature devices have a number of restrictions when applied to temperature monitoring during hyperthermia. These restrictions include small representative tissue sample of the entire tissue and tumor regions, difficulty in inserting the sensor into a deep-seated tumor, and discomfort to patients during the insertion. Because of the problems associated with invasive temperature measurement techniques, there has been a strong demand for noninvasive temperature feedback techniques such as ultrasonic imaging and microwave radiometry imaging (MRI). In addition to their focusing and real-time capabilities, ultrasound-based techniques are capable of providing satisfactory temperature resolution as well as hot-spot localization in soft tissue. MRI was applied as a noninvasive thermometry method, but it has limited temperature resolution ($\sim 0.5^\circ\text{C}$) and spatial resolution (~ 1 cm) and, therefore, can provide only an estimate of the average temperature over a certain tissue volume. Further, MRI is a costly technique, and therefore, it does not comply with the clinical requirements of treatment monitoring for tissue temperature distribution.

2.5.3 Heating Pattern Induced by Hyperthermia Applicators

Ideal Treatment Volume and Temperature Distribution. Heating pattern or specific absorption rate (SAR) induced by external devices is defined as the heat energy deposited in the tissue or tumor per second per unit mass or volume of tissue. In optimal treatment planning, it is the temperature rather than the SAR distribution that is optimized in the treatment plan. The maximum temperature generally occurs in the tissue region with heat deposition. However, one should note that SAR and temperature distribution may not have the same profile, since temperature distribution can also be affected by the environment or imposed boundary conditions.

The thermal goal of a clinically practical hyperthermia treatment is to maximize the volume of tumor tissue that is raised to the therapeutic temperature. This maximization should be accomplished while keeping the volume of normal tissue at or below some clinically specific temperature level. There are difficulties to reaching the optimal temperature distribution with the presently available heating devices. Most clinical heating systems have had such fixed power deposition patterns that optimization was limited. In recent years, the cooperation between engineers and clinicians has resulted in a new generation of heating equipment. These heating devices have considerably more flexibility in their ability to deposit power in different patterns that help reach the treatment goal. Further, the ideal temperature distribution may be achieved by manipulating the geometrical consideration or regional blood flow. In most of the transurethral microwave catheters, circulated cold water is installed in the catheter to provide protection to the sensitive prostatic urethra. Manipulation of the flow rate and temperature of the water have been demonstrated to facilitate the achievement of high temperature penetrating deep in the transition zone (Liu et al., 2000). Preheating the large arterial blood to some extent before it enters the treatment region has also been shown to improve the temperature homogeneity in that area.

Currently Used Heating Approaches. It is known that the size and location of the tumor have a significant impact on applicator design and type of heating. In most of the heating devices, heat is deposited in the tissue via electromagnetic wave absorption (microwave or radio frequency), electric conductive heating, ultrasound absorption, laser, and magnetic particles, etc. In this section, different heating devices are introduced and their advantages and limitations are described.

High energy DC shock (Scheinman et al., 1982) has been used as an implanted energy source for the treatment of drug-refractory supraventricular arrhythmias. During the catheter ablation, the peak voltage and current measured at the electrode-tissue interface are typically higher than 1000 V and 40 A, respectively. The high voltage pulse results in a very high temperature at the electrode surface. Explosive gas formation and a shock wave can occur, which may cause serious complications, including ventricular fibrillation, cardiogenic shock, and cardiac perforation.

Alternating current in the radio frequency range has been investigated as an alternative to shock for heating applicator (Huang et al., 1987; Nath et al., 1994; Nath and Haines, 1995; Wonnell et al., 1992; Zhu and Xu, 1999). Radio frequency ablation has been successfully used to treat liver neoplasms, solid renal mass, and osteoid osteomas. In recent years, this technique has been applied to destroy brain tissue for the treatment of motor dysfunctions in advanced Parkinson's disease (Kopyov et al., 1997; Linhares and Tasker, 2000; Mercello et al., 1999; Oh et al., 2001; Patel et al., 2003; Su et al., 2002). The current clinical practice of inducing RF lesions in the brain involves implanting a microelectrode-guided electrode and applying RF current to the targeted region, in order to relieve symptoms of the Parkinson's disease in patients whose symptoms cannot be controlled with traditional pharmacological treatment. RF energy is readily controllable, and the equipment is relatively cheap (Hariharan et al., 2007a). The standard RF generator used in catheter ablation produces an unmodulated sinusoidal wave alternating current at a frequency of 200 to 1000 kHz. Two electrodes are needed to attach to the tissue and a current is induced between them. The passage of current through the tissue results in resistive or ohmic heating (I^2R losses). Resistive current density is inversely proportional to the square of the distance from the electrode. Thus, resistive heating decreases with the distance from the electrode to the fourth power. Maximal power occurs within a very narrow rim of tissue surrounding the electrodes. The heating typically leads to desiccation of tissue immediately surrounding the catheter electrodes, but diverges and decreases in-between, which can cause broad variations of heating. Improved RF hyperthermia systems have been proposed to reduce the heterogeneity of the RF heating, including implanting a feedback power current system (Astrahan and Norman, 1982; Hartov et al., 1994) and using electrically insulating material around the electrodes (Cosset et al., 1986).

Microwave hyperthermia uses radiative heating produced by high-frequency power. High-frequency electromagnetic waves may be transmitted down an appropriately tuned coaxial cable and then radiated into the surrounding medium by a small antenna. The mechanism of electromagnetic heating from a microwave source is dielectric rather than ohmic. The heating is due to a propagating electromagnetic wave that raises the energy of the dielectric molecules through which the field passes by both conduction and displacement currents. While maintaining alignment with the alternating electric field, neighboring energized dipole molecules collide with each other and the electromagnetic energy is transformed into thermal energy. The main limitation of microwave heating is that the energy is absorbed within a very narrow region around the microwave antenna. Typically, the generated heat decays fast and can be approximated as proportional to $1/r^2$. The highly absorptive nature of the water content of human tissue has limited the penetration of electromagnetic energy to 1 to 2 cm.

Laser photocoagulation is a form of minimally invasive thermotherapy in which laser energy is deposited into a target tissue volume through one or more implanted optical fibers. Laser is used in medicine for incision and explosive ablation of tumors and other tissues, and for blood vessel coagulation in various tissues. Laser light is nearly monochromatic. Most popular lasers utilized in the laboratory include argon laser (488 nm), pulsed dye laser (585 to 595 nm), Nd:YAG lasers operating at 1064 nm, and diode lasers operating at 805 nm. Laser-beam power ranges from milliwatts to several watts. Usually the laser energy is focused on a small tissue area of a radius less than 300 μm , resulting in a very high heat flux. Because there is minimal penetration of laser energy into the tissue, sufficient energy is delivered to heat tissues surrounding the point of laser contact to beyond 60°C or higher, leading to denaturation and coagulation of biomolecules. Because of the high temperature elevation in the target tissue, laser photocoagulation may produce vapor, smoke, browning, and char. A char is usually formed when temperature is elevated above 225°C or higher (LeCarpentier et al., 1989; Thomsen, 1991; Torres et al., 1990; Whelan and Wyman, 1999).

Laser ablation has been used primarily in two clinical applications, one is dermatology and the other is ophthalmology. Laser treatment for port wine stain with cryogen spray cooling has been

shown as a promising clinical approach for maximizing thermal damage to the targeted blood vessels under the skin while minimizing injury to the epidermis (Jia et al., 2006). Laser use in ophthalmology has a long history. Energy absorption in the tissue or blood is largely dependent on the wavelength of the laser used; longer wavelengths penetrate more deeply into tissue than short wavelengths. Most of the laser-based treatments depend upon light/tissue interactions that occur in the superficial layers associated with the neuro-retina and retinal pigment epithelium (RPE). Conventional laser treatment for the retinal layer uses continuous or pulse wave laser (wavelength: 527 nm) with exposure time in the range of 100 to 200 ms, and power in the range of 50 to 200 mW (Banerjee et al., 2007). The laser is primarily absorbed by the melanin granules in the RPE tissue. On the other hand, in laser photocoagulation of the choroidal feeder vessels, laser energy must penetrate the overlying retinal layers, RPE, and choriocapillaris to reach the choroid and then be absorbed by the targeted feeder vessel. Considering that the targeted vessels in these studies lie relatively deep, it is logical that the widely used 805-nm-wavelength diode laser was selected as the source for maximizing energy absorption. An experimental study on pigmented rabbit eyes has shown that the photocoagulation of large choroidal arterioles can be accomplished with relatively little concomitant retinal tissue damage (Flower, 2002), when using near-infrared wavelengths, especially when used in conjunction with an injection of a biocompatible dye that enhances absorption of the laser energy. A recent theoretical simulation of the temperature field in the vicinity of the choroidal vessel has illustrated the strategy to achieve thermal damage while preserving the sensitive RPE layer (Zhu et al., 2008).

Unlike the electromagnetic heating devices mentioned above, ultrasound heating is a mechanical hyperthermic technique. The acoustic energy, when absorbed by tissue, can lead to local temperature rise. Ultrasound offers many advantages as an energy source for hyperthermia because of its small wavelength and highly controllable power deposition patterns, including penetration depth control in human soft tissue (Hariharan et al., 2007b, 2008). The depth of the resulting lesion could theoretically be increased or decreased by selecting a lower or higher ultrasound frequency, respectively. It has been shown that scanned focused ultrasound provides the ability to achieve more uniform temperature elevations inside tumors than the electromagnetic applicators. Moros and Fan (1998) have shown that the frequency of 1 MHz is not adequate for treating chest wall recurrences, since it is too penetrating. As for a deep-seated tumor (3 to 6 cm deep), longer penetration depth is achieved by using relatively low frequency (1 MHz) and/or adjusting the acoustic output power of the transducer (Moros et al., 1996). The practical problem associated with ultrasound heating is the risk of overheating the surrounding bone-tissue interface because of the high ultrasound absorption in bone.

Another hyperthermia approach involves microparticles or nanoparticles which can generate heat in tissue when subjected to an alternating magnetic field. Magnetic particle hyperthermia procedure consists of localizing magnetic particles within tumor tissue or tumor vasculature and applying an external alternating magnetic field to agitate the particles (Gilchrist et al., 1957). In this case, magnetic particles function as a heat source, which generates heat due to hysteresis loss, Néel relaxation, brownian motion, or eddy currents. Subsequently, a targeted distribution of temperature elevation can be achieved by manipulating the particle distribution in the tumor and tuning the magnetic field parameters. Compared to most conventional noninvasive heating approaches, this technique is capable of delivering adequate heat to tumor without necessitating heat penetration through the skin surface, thus avoiding the excessive collateral thermal damage along the path of energy penetration if the tumor is deep seated. In addition to treatment of deep seated tumor, the employment of nanoparticle smaller than 100 nm is especially advantageous in generating sufficient heating at a lower magnetic field strength. Typically, the particle dosage in the tumor and the magnetic field strength are carefully chosen to achieve the desired temperature elevation. Generally, the usable frequencies are in the range of 0.05 to 1.2 MHz and the field amplitude is controlled lower than 15 kA/m. Previous *in vitro* and *in vivo* studies have used a frequency in the 100 kHz range (Rand et al., 1981; Hase et al., 1989; Chan et al., 1993; Jordan et al., 1997; Hilger et al., 2001). The studies of heat generation by particles suggest that the heating characteristic of magnetic particles depends strongly on their properties, such as particle size, composition, and microstructure (Chan et al., 1993; Hergt et al., 2004; Hilger et al., 2001; Jordan et al., 1997). In particular, as the particle size decreases, thermal activation of reorientation processes leads to superparamagnetic (SPM) behavior that is capable of generating impressive levels of heating at lower field strengths. The spherical nanoparticle of 10 nm

diameter is capable of providing a specific loss power (SLP) of 211 W/g under a magnetic field of 14 kA/m in amplitude and 300 kHz in frequency. In contrast, particles with diameter of 220 nm only achieve an SLP of 144 W/g under identical conditions (Hilger et al., 2001). Therefore, nanoparticle hyperthermia provides a more effective and clinically safer therapeutic alternative for cancer treatment than microparticles.

The quantification of heat generated by the particles has suggested that the size of the individual particle and properties of the magnetic field (strength and frequency) determine its heating capacity. Hence, given the particle size and magnetic field strength, it is the spatial distribution of the particle dispersed in tissue that affects the resulting temperature elevation. However, it is not clear how the spatial concentration of the particles in the tissue correlates with the particle concentration in the carrier solution before the injection. In nanofluid transport in tissue, the injection strategy as well as interaction between particle and the porous interstitial space may affect the particle distribution. An experimental study by our group has attempted to evaluate how to achieve a spherical-shaped nanoparticle distribution in tissue. Figure 2.8 gives two images of nanoparticle distribution in agarose gel (0.2 percent) after a commercially available nanofluid was injected using a syringe pump. The selected injection rate affects significantly the final distribution of the nanofluid. As described in detail in Salloum et al. (2008a and 2008b), the ability of achieving a small spherical particle delivery is the first step to induce uniform temperature elevations in tumors with an irregular shape.

Depending on the amplitude of the magnetic field and particle dosage, the rate of temperature increase at the monitored site was as high as several degrees Celsius per minute. Temperatures up to 71°C were recorded at the tumor center (Hilger et al., 2005). The subsequent work by Johannsen and Jordan (Johannsen et al., 2005a, 2005b; Jordan et al., 2006) focused on testing the magnetic fluid hyperthermia on prostate cancer in human subjects. The histological analysis of the cancerous tissues showed a partial necrosis of the cells after the treatment. Recently, our group performed experimental study on the temperature elevation in rat muscle tissue induced by intramuscular injection of 0.2 cc nanofluid. The elevated temperatures were as high as 45°C and the FWHM (full length of half maximum) of the temperature elevation is 31 mm Salloum et al. (2008a and 2008b). All the experimental data have suggested the feasibility of elevating the tumor temperature to the desired level for tissue necrosis. However, in some tumor regions, usually at the tumor periphery, underdosage heating (temperature elevations lower than a critical value) was observed.

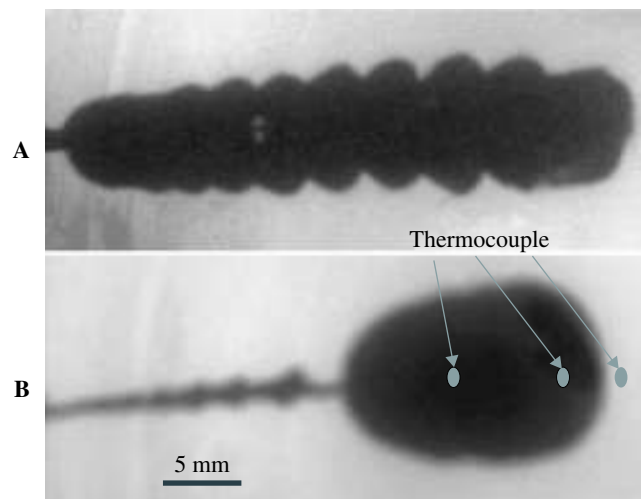


FIGURE 2.8 Two images of nanofluid distribution in agarose gel (0.2 percent). The injection rate was (a) 5 $\mu\text{L}/\text{min}$ and (b) 2.5 $\mu\text{L}/\text{min}$, respectively. The nanofluid can be viewed by the black color in the images.

Determination of SAR. Several methods are used to determine the SAR distribution induced by various heating applicators. The SAR distribution can be directly derived from the Maxwell equation of the electromagnetic field (Camart et al., 2000; Gentili et al., 1995; Ling et al., 1999; Stauffer et al., 1998; Strohhahn, 1984). The electrical field E and magnetic field B are first determined analytically or numerically from the Maxwell equation. The SAR (W/kg) is then calculated by the following equation (Sapozink et al., 1988)

$$\text{SAR} = \left(\frac{\sigma}{2\rho} \right) E^2 \quad (2.24)$$

where ρ and σ represent the density and conductivity of the media, respectively. This method is feasible when the derivation of the electromagnetic field is not very difficult. It generally requires a rather large computational resource and a long calculation time, though it is flexible for modeling the applicators and the surrounding media.

Other methods in clinical and engineering applications are experimental determination of the SAR distribution based on the heat conduction equation. The experiment is generally performed on a tissue-equivalent phantom gel. The applicability of the SAR distribution measured in the phantom gel to that in tissue depends on the electrical properties of the phantom gel. For energy absorption of ultrasound in tissue, the gel mimics tissue in terms of ultrasonic speed and attenuation/absorption properties. For heat pattern induced by microwave or radio frequency, the applicability requires that the phantom gel mimic the dielectric constant and electrical conductivity of the tissue. The electrical properties of various tissues at different wave frequencies have been studied by Stoy et al. (1982). It has been shown that in addition to the electromagnetic wave frequency, water content of the tissue is the most important factor in determining the electrical properties. Thermal properties such as heat capacity and thermal conductivity of the gel are not required if no thermal study is conducted. The ingredients of the gel can be selected to achieve the same electrical characteristics of the tissue for a specific electromagnetic wavelength. As shown in Zhu and Xu (1999), the basic ingredients of the gel used for an RF heating applicator were water, formaldehyde solution, gelatin, and sodium chloride (NaCl). Water was used to achieve a similar water content as the tissue. Formaldehyde and gelatin were the solidification agents. NaCl was added to obtain the desired electrical conductivity of tissue at that frequency. The resulted phantom gel was a semitransparent material that permits easy and precise positioning of the temperature sensors during the experimental study.

The simplest experimental approach to determining the SAR distribution is from the temperature transient at the instant of power on (Wong et al., 1993; Zhu et al., 1996b). In this approach, temperature sensors are placed at different spatial locations within the gel. Before the experiment, the gel is allowed to establish a uniform temperature distribution within the gel. As soon as the initial heating power level is applied, the gel temperature is elevated and the temperatures at all sensor locations are measured and recorded by a computer. The transient temperature field in the gel can be described by the heat conduction equation as follows:

$$\begin{aligned} \rho C \frac{\partial T}{\partial t} &= k \nabla^2 T + \text{SAR}(x, y, z) \\ t = 0 \quad T &= T_{\text{env}} \end{aligned} \quad (2.25)$$

Within a very short period after the heating power is on, heat conduction can be negligible if the phantom gel is allowed to reach equilibration with the environment before the heating. Thus, the SAR can be determined by the slope of the initial temperature rise, i.e.,

$$\text{SAR} = \rho C \left. \frac{\partial T}{\partial t} \right|_{t=0} \quad (2.26)$$

Since the SAR at each spatial location is a constant during the heating, the temperature rise at each location is expected to increase linearly if heat conduction is negligible. Figure 2.9 gives the measured temperature rise at different radial locations from an injection site of the nanofluid. Note that the

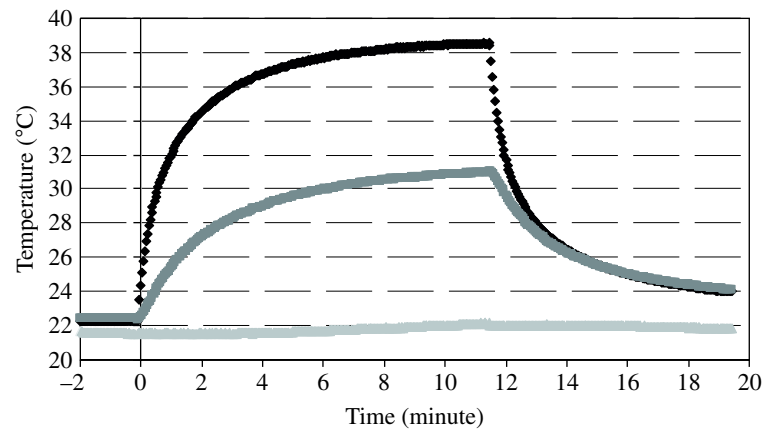


FIGURE 2.9 Initial temperature rises after heating is turned on. Temperatures are measured at three locations in the agarose gel, as shown in Fig. 2.8.

temperatures at all three probe locations were very close to each other before the heating. The temperatures increased linearly once the power was on; however, after approximately 60 seconds, the plot became curved and heat conduction within the gel was no longer negligible. For convenience the loose SAR data are generally represented by an analytic expression with several unknown parameters. Then a least-square residual fit of the SAR measurement to the analytical expression is performed to determine the unknown parameters in the expression.

It is simple to determine the SAR distribution from the initial temperature transient. This method is fairly accurate as long as the temperature is uniform before the power is turned on. However, to obtain an accurate expression for the SAR distribution, enough temperature sensors should be placed in the region where the energy is absorbed. In the situation when the SAR decays rapidly in the radial direction because of the superficial penetration of the energy, and it is difficult to place many temperature sensors in the near field, the SAR distribution must be determined by only a few measurements in the near field, which increases the measurement error.

In the experimental study by Zhu et al. (1998), the heating pattern induced by a microwave antenna was quantified by solving the inverse problem of heat conduction in a tissue equivalent gel. In this approach, detailed temperature distribution in the gel is required and predicted by solving a two-dimensional or three-dimensional heat conduction equation in the gel. In the experimental study, all the temperature probes were not required to be placed in the near field of the catheter. Experiments were first performed in the gel to measure the temperature elevation induced by the applicator. An expression with several unknown parameters was proposed for the SAR distribution. Then, a theoretical heat transfer model was developed with appropriate boundary conditions and initial condition of the experiment to study the temperature distribution in the gel. The values of those unknown parameters in the proposed SAR expression were initially assumed and the temperature field in the gel was calculated by the model. The parameters were then adjusted to minimize the square error of the deviations of the theoretically predicted from the experimentally measured temperatures at all temperature sensor locations.

2.5.4 Dynamic Response of Blood Flow to Hyperthermia

As mentioned previously, blood flow plays a profound effect in the temperature field during hyperthermia treatment. Accurately measuring and monitoring blood flow in different tissue regions and at different heating levels are especially crucial to achieve the thermal goal. The distribution of blood flow is quite heterogeneous in the tissue. Blood flow rate may be higher in the skin than in the

muscle. Blood flow in the tumor and normal tissue may also be quite different because of different vasculatures. Contrary to the general notion that blood flow is less in tumors than in normal tissues, blood flow in many tumors, particularly in small tumors, is actually greater than that in surrounding normal tissues at normothermic conditions. Even in the same tumor, blood flow generally decreases as the tumor grows larger, owing partially to progressive deterioration of vascular beds and to the rapid growth of tumor cell population relative to vascular bed.

The dynamic responses of the blood flow to hyperthermia in normal tissue and tumors are even more diversified than the blood flow heterogeneity. It is a well-known fact that heat induces a prompt increase in blood flow accompanied by dilation of vessels and an increase in permeability of the vascular wall in normal tissues. The degree of pathophysiological changes in the vascular system in normal tissue is, of course, dependent on the heating temperature, the heating duration, and the heating protocol. Experimental study by Song (1984) has shown how the vasculature changed in the skin and muscle of rodents at different time intervals after hyperthermia for varying heating temperatures at 42 to 45°C. It was shown that the blood flow in the skin increased by a factor of 4 and 6 upon heating at 43°C for 60 and 120 minutes, respectively. At 44°C the skin blood flow was about 12 times the control value within 30 minutes. At high heating temperature, there existed a critical time after which the blood flow decreased because of vasculature damage. This critical time was more quickly reached when the heating temperature was higher. The blood flow increase in the muscle was similar to that observed in the skin layer, a tenfold increase in the blood flow was noticed at the 45°C heating.

An indisputable fact emerging from various experimental data indicates that heat-induced change in the blood flow in some tumors is considerably different from that in normal tissue. As noted in Fig. 2.10, there was a limited increase in blood flow in tumors during the initial heating period (Song, 1984). When the heating was prolonged, the tumor blood flow decreased progressively. The different responses of the normal tissue and tumors suggest the feasibility of selective tumor heating. A relatively small increase in blood flow in tumors favors retention of heat within the tumor volume, and thus causes greater heat damage. On the other hand, a large blood flow increase in the normal tissue by vascular dilation causes tissue cooling and high survival of cells.

Since blood flow is the major route of heat dissipation during hyperthermia, attempts have been made to modify the vascular responses in tumors and normal tissue to heat (Reinhold and Endrich,

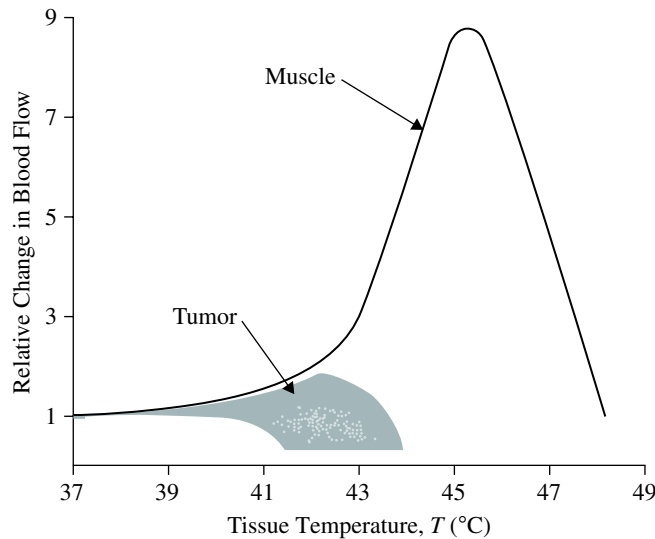


FIGURE 2.10 Temperature-dependent changes in the relative blood perfusion rates for muscle and animal tumors. [From Song (1984), with permission.]

1986; Song, 1991). Decreased tumor perfusion may induce changes in the tumor microenvironment, such as reduced pH value and energy supply, thus enhance the thermal cytotoxicity (Gerweck, 1977; Overgaard, 1976; Song et al., 1994). An injection of hydralazine to dogs was reported to decrease the blood flow by 50 percent in the tumor and increase the blood flow in the underlying muscle by a factor of three (Song, 1984). It was demonstrated that the use of vasoactive drugs led to intracellular acidification of the tumor environment (Song et al., 1994). It has been shown that 1 hour after an intravenous or intraperitoneal injection of KB-R8498, the blood flow in the SCK mammary carcinoma tumors of mice was reduced 30 to 60 percent (Griffin et al., 1998; Ohashi et al., 1998). The effect has also been made to induce a blood flow increase in the normal tissue. It was reported that preferentially dilating vessels in normal tissues using vasodilator such as sodium nitroprusside led to shunting of blood away from the tumor, and thus reducing the cooling effect of the blood flow in a tumor during local hyperthermia (Jirtle, 1988; Prescott et al., 1992). Not surprisingly, radiation also altered the response of vasculatures to heat. It was reported that irradiation with 2000 R given 1 hour before heating at 42°C for 30 minutes, enhanced the heat-induced vascular damage in the cervical carcinoma of hamsters. Another research showed that hyperthermia of 42°C for 1 hour, given several weeks after irradiation, enhanced the capacity of blood flow increase in skin and muscle (Song, 1984).

It has been increasingly evident that the response of vascular beds to heat in tumors differs considerably from that in normal tissues. The effective clinical use of hyperthermia depends on a careful application of these biological principles emerging from experimental work. More experimental measurements of temperature response are needed for different tumor types at different ages. It is also important to evaluate the applicability of the dynamic response measured in animal to human subjects. Another issue to be addressed is the hyperthermia-induced blood flow change in drug delivery, since the reduced tumor blood flow may decrease the drug delivered to the tumors.

2.5.5 Theoretical Modeling

In treatment planning, quantitative three-dimensional thermal modeling aids in the identification of power delivery for optimum treatment. Thermal modeling provides the clinician with powerful tools that improve the ability to deliver safe and effective therapy, and permits the identification of critical monitoring sites to assess tumor heating as well as to ensure patient safety. Thermal modeling maximizes the information content of (necessarily sparse) invasive thermometry. The empirical temperature expression (if it is possible) can be used to develop an online reference for monitoring tissue temperatures and building a feedback control of the applied power to avoid overheating in critical tissue areas during the hyperthermia therapy.

Tissue temperature distributions during hyperthermia treatments can be theoretically determined by solving the bioheat transfer equation (continuum model or vascular model), which considers the contributions of heat conduction, blood perfusion, and external heating. In addition to geometrical parameters and thermal properties, the following knowledge must be determined before the simulation. The SAR distribution induced by the external heating device should be determined first. The regional blood perfusion in the tissue and tumor and their dynamic responses to heating are also required. All this information, with appropriate boundary and initial conditions, allows one to calculate the temperature distribution of the tissue.

Analytical solution for the temperature field during the hyperthermia treatment is available for certain tissue geometries (Liu et al., 2000; Zhu and Xu, 1999). In most of the situations, temperature field is solved by numerical methods because of the irregular tissue geometry and complicated dynamic response of blood flow to heating (Chatterjee and Adams, 1994; Charny et al., 1987; Clegg and Roamer, 1993; Zhu et al., 2008a, 2008b).

Parametric studies can be performed to evaluate the influence of different parameters, such as heating level, tissue perfusion, and cooling fluid, on the temperature elevation. Extensive parametric studies can be performed quickly and inexpensively so that sensitive (and insensitive) parameters can be identified, systems can be evaluated, and critical experiments can be identified. This is especially important when the parameter is unknown. It is also possible to extract the ideal SAR distribution

from the parametric study (Loulou and Scott, 2000) and design an improved heating applicator in future. Knowledge of the expected thermal profiles could be used to guide experimental and clinical studies in using an optimum thermal dose to achieve a desired therapeutic effect. The optimal thermal dose needed in the treatment volume predicted by the theory helps physicians to evaluate the effectiveness of the heating devices and their treatment protocols.

REFERENCES

- Arkin, H., Holmes, K. R., Chen, M. M., and Bottje, W. G., 1986, "Thermal Pulse Decay Method for Simultaneous Measurement of Local Thermal Conductivity and Blood Perfusion: A Theoretical Analysis," *ASME Journal of Biomechanical Engineering*, **108**:208–214.
- Arkin, H., Holmes, K. R., and Chen, M. M., 1987, "Computer Based System for Continuous On-Line Measurements of Tissue Blood Perfusion," *Journal of Biomedical Engineering*, **9**:38–45.
- Astrahan, M. A., and Norman, A., 1982, "A Localized Current Field Hyperthermia System for Use with 192 Iridium Interstitial Implants," *Medical Physics*, **9**:419–424.
- Aurer, C., and Carpenter, D. O., 1980, "Choroidal Blood Flow as a Heat Dissipating Mechanism in the Macula," *American Journal of Ophthalmology*, **89**:641–646.
- Baish, J. W., 1994, "Formulation of a Statistical Model of Heat Transfer in Perfused Tissue," *ASME Journal of Biomechanical Engineering*, **116**:521–527.
- Banerjee, R. K., Zhu, L., Gopalakrishnan, P., and Kazmierczak, M. J., 2007, "Influence of Laser Parameters on Selective Retinal Treatment Using Single-Phase Heat Transfer Analyses," *Medical Physics*, **34**(5):1828–1841.
- Bazett, H. C., 1941, "Temperature Sense in Men," In: *Temperature: Its Measurement and Control in Science and Industry*, New York: Reinhold, pp. 489–501.
- Borgos, J., 1996, "Laser Doppler Monitoring of Cerebral Blood Flow," *Neurological Research*, **18**:251–255.
- Brinck, H., and Werner, J., 1994, "Estimation of the Thermal Effect of Blood Flow in a Branching Countercurrent Network Using a Three-Dimensional Vascular Model," *ASME Journal of Biomechanical Engineering*, **116**:324–330.
- Camart, J. C., Desprez, D., Prevost, B., Sozanski, J. P., Chive, M., and Pribetich, J., 2000, "New 434 MHz Interstitial Hyperthermia System Monitored by Microwave Radiometry: Theoretical and Experimental Results," *International Journal of Hyperthermia*, **16**:95–111.
- Cetas, T. C., Conner, W. G., and Manning, M. R., 1980, "Monitoring of Tissue Temperature During Hyperthermia Therapy," *Annals of the New York Academy of Sciences*, **335**:281–297.
- Chan, D. C. F., Kirpotin, D. B., and Bunn, P. A., 1993, "Synthesis and Evaluation of Colloidal Magnetic Iron Oxides for the Site-Specific Radio Frequency-Induced Hyperthermia of Cancer," *Journal of Magnetism and Magnetic Materials*, **122**:374–378.
- Charny, C. K., Hagmann, M. J., and Levin, R. L., 1987, "A Whole Body Thermal Model of Man during Hyperthermia," *IEEE Transactions on Biomedical Engineering*, **34**(5):375–387.
- Charny, C. K., Weinbaum, S., and Levin, R. L., 1990, "An Evaluation of the Weinbaum-Jiji Bioheat Equation for Normal and Hyperthermic Conditions," *ASME Journal of Biomechanical Engineering*, **112**:80–87.
- Chato, J. 1980, "Heat Transfer to Blood Vessels," *ASME J. Biomech. Eng.*, **102**:110–118.
- Chatterjee, I. and Adams, R. E., 1994, "Finite Element Thermal Modeling of the Human Body under Hyperthermia Treatment for Cancer," *International Journal of Computer applications in Technology*, **7**:151–159.
- Chen, M. M., and Holmes, K. R., 1980, "Microvascular Contributions to Tissue Heat Transfer," *Annals of the New York Academy of Science*, **335**:137–150.
- Clark, R. S., Kochanek, P. M., Marion, D. W., Schiding, J. K., White, M. Palmer, A. M., and DeKosky, S. T., 1996, "Mild Posttraumatic Hypothermia Reduces Mortality after Severe Controlled Cortical Impact in Rats," *Journal of Cerebral Blood Flow & Metabolism*, **16**(2):253–261.
- Clegg, S. T., and R. B. Roemer, 1993, "Reconstruction of Experimental Hyperthermia Temperature Distributions: Application of State and Parameter Estimation," *ASME Journal of Biomechanical Engineering*, **115**:380–388.
- Cosset, J. M., Dutreix, J., Haie, C., Mabire, J. P., and Damia, E., 1986, "Technical Aspects of Interstitial Hyperthermia," In: *Recent Results in Cancer Research*, vol. 101, Berlin, Heidelberg: Springer Publishers, 56–60.

- Crezee, J., and Lagendijk, J. J. W., 1990, "Experimental Verification of Bioheat Transfer Theories: Measurement of Temperature Profiles around Large Artificial Vessels in Perfused Tissue," *Physics in Medicine and Biology*, **35**(7):905–923.
- Crezee, J., Mooibroek, J., Bos, C. K., and Lagendijk, J. J. W., 1991, "Interstitial Heating: Experiments in Artificially Perfused Bovine Tongues," *Physics in Medicine and Biology*, **36**:823–833.
- Dewhirst, M. W., Prosnitz, L., Thrall, D., Prescott, D., Clegg, S., Charles, C., MacFall, J., et al., 1997, "Hyperthermia Treatment of Malignant Diseases: Current Status and a View Toward the Future," *Seminars in Oncology*, **24**(6):616–625.
- Dorr, L. N., and Hynynen, K., 1992, "The Effects of Tissue Heterogeneities and Large Blood Vessels on the Thermal Exposure Induced by Short High-Power Ultrasound Pulses," *International Journal of Hyperthermia*, **8**:45–59.
- Engelhart, M., and Kristensen, J. K., 1986, "Raynaud's Phenomenon: Blood Supply to Fingers During Indirect Cooling, Evaluated by Laser Doppler Flowmetry," *Clinical Physiology*, **6**:481–488.
- Firorini, A., Fumero, R., and Marchesi, R., 1982, "Cardio-Surgical Thermography," *Proceedings of SPIE*, **359**:249.
- Flower, R. W., 2002, "Optimizing Treatment of Choroidal Neovascularization Feeder Vessels Associated with Age-Related Macular Degeneration," *American Journal of Ophthalmology*, **134**:228–239.
- Fu, G., "A Transient 3-D Mathematical Thermal Model for the Clothed Human," Ph.D. Dissertation, Kansas State University, 1995.
- Gautherie, M., and Gros, C. M., 1980, "Breast Thermography and Cancer Risk Prediction," *Cancer*, **45**(1):51–56.
- Gentil, G. B., Lenocini, M., Tremblay, B. S., Schweizer, S. E., 1995, "FDTD Electromagnetic and Thermal Analysis of Interstitial Hyperthermic Applicators: Finite-Difference Time-domain," *IEEE Transactions on Biomedical Engineering*, **42**(10):973–980.
- Gerweck, L. E., 1977, "Modification of Cell Lethality at Elevated Temperatures: The pH Effect," *Radiation Research*, **70**:224–235.
- Gilchrist, R. K., Medal, R., Shorey, W. D., Hanselman, R. C., Parrott, J. C., and Taylor, C. B., 1957, "Selective Inductive Heating of Lymph Nodes," *Annals of Surgery*, **146**:596–606.
- Griffin, R. J., Ogawa, A., Shakil, A., and Song, C. W., 1998, "Local Hyperthermia Treatment of Solid Tumors: Interplay between Thermal Dose and Physiological Parameters," ASME, HTD-Vol. 362, *Advances in Heat and Mass Transfer in Biological Systems*, pp. 67–69.
- Hariharan, P., Chang, I., Myers, M., and Banerjee, R. K., 2007a, "Radio Frequency (RF) Ablation in a Realistic Reconstructed Hepatic Tissue," *ASME Journal of Biomechanical Engineering*, **129**:354–364.
- Hariharan, P., Myers, M. R., and Banerjee, R. K., 2007b, "HIFU Procedures at Moderate Intensities—Effect of Large Blood Vessels," *Physics in Medicine and Biology*, **52**:3493–3513.
- Hariharan, P., Myers, M. R., Robinson, R., Maruyada, S., Sliva, J., and Banerjee, R. K., 2008, "Characterization of High Intensity Focused Ultrasound Transducers Using Acoustic Streaming," *Journal of Acoustical Society of America*, in press.
- Hartov, A., Colacchio, T. A., Hoopes, P. J., and Strohbehn, J. W., 1994, "The Control Problem in Hyperthermia," ASME HTD-Vol. 288, *Advances in Heat and Mass Transfer in Biological Systems*, pp. 119–126.
- Hase, M., Sako, M., Fujii, M., Ueda, E., Nagae, T., Shimizu, T., Hirota, S., and Kono, M., 1989, "Experimental Study of Embolohyperthermia for the Treatment of Liver Tumors by Induction Heating to Ferromagnetic Particles Injected into Tumor Tissue," *Nippon Acta Radiologica*, **49**:1171–1173.
- He, Q., Zhu, L., Weinbaum, S., and Lemons, D. E., 2002, "Experimental Measurements of Temperature Variations along Paired Vessels from 200 to 1000 (m in Diameter in Rat Hind Leg)," *ASME Journal of Biomedical Engineering*, **124**:656–661.
- He, Q., Zhu, L., and Weinbaum, S., 2003, "Effect of Blood Flow on Thermal Equilibration and Venous Rewarming," *Annals of Biomedical Engineering*, **31**:659–666.
- Head, J. F., Wang, F., and Elliott R. L., 1993, "Breast Thermography Is a Noninvasive Prognostic Procedure That Predicts Tumor Growth Rate in Breast Cancer Patients," *Annals of the New York Academy of Sciences*, **698**:153–158.
- Hergt, R., Hiergeist, R., Zeisberger, M., Glockl, G., Weitschies, W., Ramirez, L. P., Hilger, I., and Kaiser, W. A., 2004, "Enhancement of AC-Losses of Magnetic Nanoparticles for Heating Applications," *Journal of Magnetism and Magnetic Materials*, **280**:358–368.
- Hilger, I., Andra, W., Hergt, R., Hiergeist, R., Schubert, H., and Kaiser, W. A., 2001, "Electromagnetic Heating of Breast Tumors in Interventional Radiology: in vitro and in vivo Studies in Human Cadavers and Mice," *Radiology*, **218**:570–575.

- Hilger, I., Hergt, R., and Kaiser, W. A., 2005, "Towards Breast Cancer Treatment by Magnetic Heating," *Journal of Magnetism and Magnetic Materials*, **293**:314–319.
- Holmes, K. R., 1997, "Biological Structures and Heat Transfer," In: *Report from the Allerton Workshop on the Future of Biothermal Engineering*, pp. 14–37.
- Hu, L., Gupta, A., Gore, J. P., and Xu, L. X., 2004, "Effect of Forced Convection on the Skin Thermal Expression of Breast Cancer," *Journal of Biomechanical Engineering*, **126**(2):204–211.
- Huang, S. K., Bharati, S., Graham, A. R., Lev, M., Marcus, F. I., and Odell, R. C., 1987, "Closed Chest Catheter Desiccation of the Atrioventricular Junction Using Radiofrequency Energy—A New Method of Catheter Ablation," *Journal of the American College of Cardiology*, **9**:349–358.
- Jamieson, S. W., Kapelanski, D. P., Sakakibara, N., Manecke, G. R., Thistlethwaite, P. A., Kerr, K. M., Channick, R. N., Fedullo, P. F., and Auger, W. R., 2003, "Pulmonary Endarterectomy: Experience and Lessons Learned in 1,500 Cases," *Annals of Thoracic Surgery*, **76**(5):1457–1462.
- Jia, W., Aguilar, G., Verkrusse, W., Franco, W., and Nelson, J. S., 2006, "Improvement of Port Wine Stain Laser Therapy by Skin Preheating Prior to Cryogen Spray Cooling: A Numerical Simulation," *Lasers in Surgery and Medicine*, **38**:155–162.
- Jirtle, R. L., 1988, "Chemical Modification of Tumor Blood Flow," *International Journal of Hyperthermia*, **4**:355–371.
- Johannsen, M., Gneveckow, U., Eckelt, L., Feussner, A., Waldofner, N., Scholz, R., Deger, S., Wust, P., Loening, S. A., Jordan A., 2005a, "Clinical Hyperthermia of Prostate Cancer Using Magnetic Nanoparticles: Presentation of a New Interstitial Technique," *International Journal of Hyperthermia*, **21**:637–647.
- Johannsen, M., Thiesen, B., Jordan, A., Taymoorian, K., Gneveckow, U., Waldofner, N., Scholz, R., et al., 2005b, "Magnetic Fluid Hyperthermia (MFH) Reduces Prostate Cancer Growth in the Orthotopic Dunning R3327 Rat Model," *Prostate*, **64**:283–292.
- Jones, B. F., 1998, "A Reappraisal of the Use of Infrared Thermal Image Analysis in Medicine," *IEEE Transactions on Medical Imaging*, **17**(6):1019–1027.
- Jordan, A., Scholz, R., Wust, P., Fahling, H., Krause, J., Wlodarczyk, W., Sander, B., Vogl, T., and Felix, R., 1997, "Effects of Magnetic Fluid Hyperthermia (MFH) on C3H Mammary Carcinoma in vivo," *International Journal of Hyperthermia*, **13**(6):587–605.
- Jordan, A., Scholz, R., Maier-Hauff, K., Van Landeghem, F. K., Waldofner, N., Teichgraaber, U., Pinkernelle, J., et al., 2006, "The Effect of Thermotherapy Using Magnetic Nanoparticles on Rat Malignant Glioma," *Journal of Neuro-Oncology*, **78**:7–14.
- Kopyov, O., Jacques, D., Duma, C., Buckwalter, G., Kopyov, A., Lieberman, A., and Copcutt, B., 1997, "Microelectrode-Guided Posteroventral Medial Radiofrequency Pallidotomy For Parkinson's Disease," *Journal of Neurosurgery*, **87**:52–55.
- Lam, J. M. K., Hsiang, J. N. K., and Poon, W. S., 1997, "Monitoring of Autoregulation Using Laser Doppler Flowmetry in Patients with Head Injury," *Journal of Neurosurgery*, **86**:438–455.
- Lapayowker, M. S., and Revesz, G., 1980, "Thermography and Ultrasound in Detection and Diagnosis of Breast Cancer," *Cancer*, **46**(4 suppl):933–938.
- LeCarpentier, G. L., Motamedi, M., McMath, L. P., Rastegar, S., and Welch, A. J., 1989, "The Effect of Wavelength on Ablation Mechanism during cw Laser Irradiation: Argon Verses Nd:YAG (1.32 μm)," *Proceedings of the 11th Annual IEEE Engineering in Medicine and Biology Society Conference*, pp. 1209–1210.
- Lemons, D. E., Chien, S., Crawshaw, L. I., Weinbaum, S., and Jiji, L. M., 1987, "The Significance of Vessel Size and Type in Vascular Heat Transfer," *American Journal of Physiology*, **253**:R128–R135.
- Ling, J. X., Hand, J. W., and Young, I. R., 1999, "Effect of the SAR Distribution of a Radio Frequency (RF) Coil on the Temperature Field Within a Human Leg: Numerical Studies," ASME HTD-Vol. 363, *Advances in Heat and Mass Transfer in Biotechnology*, pp. 1–7.
- Linhares, M. N., and Tasker, R. R., 2000, "Microelectrode-Guided Thalamotomy for Parkinson's Disease," *Neurosurgery*, **46**:390–398.
- Liu, J., Zhu, L., and Xu, L. X., 2000 "Studies on the Three-Dimensional Temperature Transients in the Canine Prostate during Transurethral Microwave Thermal Therapy," *ASME Journal of Biomechanical Engineering*, **122**:372–379.
- Loulou, T., and Scott, E. P., "2-D Thermal Dose Optimization in High Intensity Focused Ultrasound Treatments Using the Adjoint Method," ASME HTD-Vol. 368/BED-Vol. 47, *Advances in Heat and Mass Transfer in Biotechnology – 2000*, pp. 67–71.

- Marion, D. W., Leonov, Y., Ginsberg, M., Katz, L. M., Kochanek, P. M., Lechleuthner, A., Nemoto, E. M., et al., 1996, "Resuscitative Hypothermia," *Critical Care Medicine*, **24**(2):S81–S89.
- Marion, D. W., Penrod, L. E., Kelsey, S. F., Obrist, W. D., Kochanek, P. M., Palmer, A. M., Wisniewski, S. R., and DeKosky, S. T., 1997, "Treatment of Traumatic Brain Injury with Moderate Hypothermia," *New England Journal of Medicine*, **336**:540–546.
- Matsukawa, T., Ozaki, M., Hanagata, K., Iwashita H., Miyaji, T., and Kumazawa, T., 1996, "A Comparison of Four Infrared Tympanic Thermometers with Tympanic Membrane Temperatures Measured by Thermocouples," *Canadian Journal of Anesthesia*, **43**(12):1224–1228.
- Merello, M., Nouzeilles, M. I., Kuzis, G., Cammarota, A., Sabe, L., Betti, O., Starkstein, S., and Leiguarda, R., 1999, "Unilateral Radiofrequency Lesion versus Electrostimulation of Posteroventral Pallidum: A Prospective Randomized Comparison," *Movement Disorders*, **14**:50–56.
- Moros, E. G., Fan, X., and Straube, W. L., 1996, "Penetration Depth Control with Dual Frequency Ultrasound," ASME HTD-Vol. 337/BED-Vol. 34, *Advances in Heat and Mass Transfer in Biotechnology*, pp. 59–65.
- Moros, E. G., and Fan, X., 1998, "Model for Ultrasonic Heating of Chest Wall Recurrences," ASME HTD-Vol. 362/BED-Vol. 40, *Advances in Heat and Mass Transfer in Biotechnology*, pp. 27–33.
- Myrhae, R., and Eriksson, E., 1984, "Arrangement of the Vascular Bed in Different Types of Skeletal Muscles," *Prog. Appl. Microcirc.*, **5**:1–14.
- Nath, S., DiMarco, J. P., and Haines, D. E., 1994, "Basic Aspect of Radio Frequency Catheter Ablation," *Journal of Cardiovascular Electrophysiology*, **5**:863–876.
- Nath, S., and Haines, D. E., 1995, "Biophysics and Pathology of Catheter Energy Delivery System," *Progress in Cardiovascular Diseases*, **37**(4):185–204.
- Nussmeier, N. A., 2002, "A Review of Risk Factors for Adverse Neurological Outcome after Cardiac Surgery," *Journal of Extracorporeal Technology*, **34**:4–10.
- Obeid, A. N., Barnett, N. J., Dougherty, G., and Ward, G., 1990, "A Critical Review of Laser Doppler Flowmetry," *Journal of Medical Engineering and Technology*, **14**(5):178–181.
- Oh, M. Y., Hodaie, M., Kim, S. H., Alkhani, A., Lang, A. E., and Lozano, A. M., 2001, "Deep Brain Stimulator Electrodes Used for Lesioning: Proof of Principle," *Neurosurgery*, **49**:363–369.
- Ohashi, M., Matsui, T., Sekida, T., Idogawa, H., Matsugi, W., Oyama, M., Naruse, K., et al., 1998, "Anti-tumor Activity of a Novel Tumor Blood Flow Inhibitor, KB-R8498," *Proceedings of the American Association for Cancer Research*, **39**:312.
- Overgaard, J., 1976, "Influence of Extracellular pH on the Viability and Morphology of Tumor Cells Exposed to Hyperthermia," *Journal of National Cancer Institute*, **56**:1243–1250.
- Overgaard, J., 1987, "Some Problems Related to the Clinical Use of Thermal Isoeffect Doses," *International Journal of Hyperthermia*, **3**:329–336.
- Parker, W. J., Jenkins, R. J., Butler, C. P., and Abbott, G. L., 1961, "Flash Method of Determining Thermal Diffusivity, Heat Capacity, and Thermal Conductivity," *Journal of Applied Physics*, **32**:1679–1684.
- Parker, D. L., Smith, V., Sheldon, P., Crooks, L. E., and Fussell, L., 1982, "Temperature Distribution Measurements in Two-Dimensional NMR Imaging," *Medical Physics*, **10**(3):321–325.
- Patel, N. K., Heywood, P., O'Sullivan, K., McCarter, R., Love, S., and Gill, S. S., 2003, "Unilateral Subthalamotomy in the Treatment of Parkinson's Disease," *Brain*, **126**:1136–1145.
- Pennes, H. H., 1948, "Analysis of Tissue and Arterial Blood Temperatures in the Resting Human Forearm," *Journal of Applied Physiology*, **1**:93–122.
- Prescott, D. M., Samulski, T. V., Dewhurst, M. W., Page, R. L., Thrall, D. E., Dodge, R. K., and Oleson, J. R., 1992, "Use of Nitroprusside to Increase Tissue Temperature during Local Hyperthermia in Normal and Tumor-Bearing Dogs," *International Journal of Radiation Oncology Biology Physics*, **23**:377–385.
- Raaymakers, B. W., Crezee, J., and Lagendijk, J. J. W., 2000, "Modeling Individual Temperature Profiles from an Isolated Perfused Bovine Tongue," *Physics in Medicine and Biology*, **45**:765–780.
- Rand, R. W., Snow, H. D., Elliott, D. G., and Snyder, M., 1981, "Thermomagnetic Surgery for Cancer," *Applied Biochemistry and Biotechnology*, **6**:265–272.
- Reinhold, H. S., and Endrich, B., 1986, "Tumor Microcirculation as a Target for Hyperthermia," *International Journal of Hyperthermia*, **2**:111–137.

- Reith, J., Jorgensen, H. S., Pedersen, P. M., Nakayama, H., Raaschou, H. O., Jeppesen, L. L., and Olsen, T. S., 1996, "Body Temperature in Acute Stroke: Relation to Stroke Severity, Infarct Size, Mortality, and Outcome," *Lancet*, **347**:422–425.
- Roemer, R. B., 1990, "Thermal Dosimetry," In: *Thermal Dosimetry and Treatment Planning*, edited by M. Gaytherie, Berlin: Springer, pp. 119–214.
- Salloum, M. D., 2005, "A New Transient Bioheat Model of the Human Body and Its Integration to Clothing Models," M.S. Thesis, American University of Beirut.
- Salloum, M., Ma, R., Weeks, D., and Zhu, L., 2008a, "Controlling Nanoparticle Delivery in Magnetic Nanoparticle Hyperthermia for Cancer Treatment: Experimental Study in Agarose Gel," *International Journal of Hyperthermia*, **24**(4):337–345.
- Salloum, M., Ma, R., and Zhu, L., 2008b, "An In-Vivo Experimental Study of the Temperature Elevation in Animal Tissue during Magnetic Nanoparticle Hyperthermia," *International Journal of Hyperthermia*, **24**(7):589–601.
- Sapozink, M. D., Cetas, T., Corry, P. M., Egger, M. J., Fessenden, P., and The NCI Hyperthermia Equipment Evaluation Contractors' Group, 1988, "Introduction to Hyperthermia Device Evaluation," *International Journal of Hyperthermia*, **4**:1–15.
- Schabauer, A. M. A., and Rooke, T. W., 1994, "Cutaneous Laser Doppler Flowmetry: Applications and Findings," *Mayo Clinic Proceedings*, **69**:564–574.
- Scheinman, M. M., Morady, F., Hess, D. S., and Gonzalez, R., 1982, "Catheter-Induced Ablation of the Atrioventricular Junction to Control Refractory Supraventricular Arrhythmias," *JAMA*, **248**:851–855.
- Shibasaki, M., Kondo, N., Tominaga, H., Aoki, K., Hasegawa, E., Idota, Y., and Moriwaki, T., 1998, "Continuous Measurement of Tympanic Temperature with a New Infrared Method Using an Optical Fiber," *Journal of Applied Physiology*, **85**(3):921–926.
- Smith, C. E., 1991, "A Transient Three-Dimensional Model of the Thermal System," Ph.D. Dissertation, Kansas State University.
- Smits, G. J., Roman, R. J., and Lombard, J. H., 1986, "Evaluation of Laser-Doppler Flowmetry as a Measure of Tissue Blood Flow," *Journal of Applied Physiology*, **61**(2):666–672.
- Song, C. W., 1984, "Effect of Local Hyperthermia on Blood Flow and Microenvironment: A Review," *Cancer Research*, **44**:4721s–4730s.
- Song, C. W., 1991, "Role of Blood Flow in Hyperthermia," In: *Hyperthermia and Oncology*, M. Urano and E. B. Douple, eds., VSP Publishers, Utrecht, The Netherlands, **3**:275–315.
- Song, C. W., Kim, G. E., Lyons, J. C., Makepeace, C. M., Griffin, R. J., Rao, G. H., and Cragon, E. J. Jr., 1994, "Thermosensitization by Increasing Intracellular Acidity with Amiloride and Its Analogs," *International Journal of Radiation Oncology Biology Physics*, **30**:1161–1169.
- Stauffer, P. R., Rossetto, F., Leoncini, M., and Gentili, G. B., 1998, "Radiation Patterns of Dual Concentric Conductor Microstrip Antennas for Superficial Hyperthermia," *IEEE Transactions on Biomedical Engineering*, **45**(5):605–613.
- Stoy, R. D., Foster, K. R., and Schwan, H. P., 1982, "Dielectric Properties of Mammalian Tissues from 0.1 to 100 MHz: A Summary of Recent Data," *Physics in Medicine and Biology*, **27**:501–513.
- Strohbehn, J. W., 1984, "Calculation of Absorbed Power in Tissue for Various Hyperthermia Devices," *Cancer Research*, **44**(supp 1):4781s–4787s.
- Su, P. C., Tseng, H-M., Liu, H-M., Yen, R-F., and Liou, H-H., 2002, "Subthalamotomy for Advanced Parkinson's Disease," *Journal of Neurosurgery*, **97**:598–606.
- Thomsen, S., 1991, "Pathologic Analysis of Photothermal and Photomechanical Effects of Laser-Tissue Interactions," *Photochemistry and Photobiology*, **53**:825–835.
- Torres, J. H., Motamedi, M., and Welch, A. J., 1990, "Disparate Absorption of Argon Laser Radiation by Fibrous Verses Fatty Plaque: Implications for Laser Angioplasty," *Lasers in Surgery and Medicine*, **10**:149–157.
- Wagner, K. R., and Zuccarello, M., 2005, "Local Brain Hypothermia for Neuroprotection in Stroke Treatment and Aneurysm Repair," *Neurological Research*, **27**:238–245.
- Wass, C. T., Lanier, W. L., Hofer, R. E., Scheithauer, B. W., and Andrews, A. G., 1995, "Temperature Changes of 1(C Alter Functional Neurological Outcome and Histopathology in a Canine Model of Complete Cerebral Ischemia," *Anesthesia*, **83**:325–335.
- Weinbaum, S., Jiji, L. M., and Lemons, D. E., 1984, "Theory and Experiment for the Effect of Vascular Microstructure on Surface Tissue Heat Transfer—Part I: Anatomical Foundation and Model Conceptualization," *ASME Journal of Biomechanical Engineering*, **106**:321–330.

- Weinbaum, S., and Jiji, L. M., 1985, "A New Simplified Bioheat Equation for the Effect of Blood Flow on Local Average Tissue Temperature," *Journal of Biomechanical Engineering*, **107**:131–139.
- Weinbaum, S., Xu, L. X., Zhu, L., and Ekpen, A., 1997, "A New Fundamental Bioheat Equation for Muscle Tissue: Part I—Blood Perfusion Term," *ASME Journal of Biomechanical Engineering*, **119**:278–288.
- Whelan, W. M., and Wyman, D. R., 1999, "A Model of Tissue Charring during Interstitial Laser Photocoagulation: Estimation of the Char Temperature," ASME HTD-Vol. 363/BED-Vol. 44, *Advances in Heat and Mass Transfer in Biotechnology*, pp. 103–107.
- Whitmore, R. L., 1968, *Rheology of Circulation*, Pergamon Press, London.
- Wissler, E. H., 1985, "Mathematical Simulation of Human Thermal Behavior Using Whole Body Models," Chapter 13, In: *Heat and Mass Transfer in Medicine and Biology*, New York: Plenum Press, pp. 325–373.
- Wissler, E. H., 1998, "Pennes' 1948 Paper Revisited," *Journal of Applied Physiology*, **85**:35–41.
- Wong, T. Z., Jonsson, E., Hoopes, P. J., Trembly, B. S., Heaney, J. A., Duple, E. B., and Coughlin, C. T., 1993, "A Coaxial Microwave Applicator for Transurethral Hyperthermia of the Prostate," *The Prostate*, **22**:125–138.
- Wonnell, T. L., Stauffer, P. R., and Langberg, J. J., 1992, "Evaluation of Microwave and Radio Frequency Catheter Ablation in a Myocardium-Equivalent Phantom Model," *IEEE Transaction in Biomedical Engineering*, **39**:1086–1095.
- Xu, L. X., Chen, M. M., Holmes, K. R., and Arkin, H., 1991, "The Theoretical Evaluation of the Pennes, the Chen-Holmes and the Weinbaum-Jiji Bioheat Transfer Models in the Pig Renal Cortex," ASME WAM, Atlanta, HTD-Vol. 189, pp. 15–22.
- Xu, L. X., Chen, M. M., Holmes, K. R., and Arkin, H., 1993, "Theoretical Analysis of the Large Blood Vessel Influence on the Local Tissue Temperature Decay after Pulse Heating," *ASME Journal of Biomechanical Engineering*, **115**:175–179.
- Xu, L. X., Zhu, L., and Holmes, K. R., 1998, "Thermoregulation in the Canine Prostate during Transurethral Microwave Hyperthermia, Part I: Temperature Response," *International Journal of hyperthermia*, **14**(1):29–37.
- Xu, L. X., and Anderson, G. T., 1999, "Techniques for Measuring Blood Flow in the Microvascular Circulation," Chapter 5, In: *Biofluid Methods and Techniques in Vascular, Cardiovascular, and Pulmonary Systems*, vol. 4, Gordon and Breach Science Publisher, Newark.
- Zhu, L., Lemons, D. E., and Weinbaum, S., 1995, "A New Approach for Prediction the Enhancement in the Effective Conductivity of Perfused Muscle Tissue due to Hyperthermia," *Annals of Biomedical Engineering*, **23**:1–12.
- Zhu, L., Weinbaum, S., and Lemons, D. E., 1996a, "Microvascular Thermal Equilibration in Rat Cremaster Muscle," *Annals of Biomedical Engineering*, **24**:109–123.
- Zhu, L., Xu, L. X., Yuan, D. Y., and Rudie, E. N., 1996b, "Electromagnetic (EM) Quantification of the Microwave Antenna for the Transurethral Prostatic Thermotherapy," ASME HTD-Vol. 337/BED-Vol. 34, *Advances in Heat and Mass Transfer in Biotechnology*, pp. 17–20.
- Zhu, L., Xu, L. X., and Chencinski, N., 1998, "Quantification of the 3-D Electromagnetic Power Absorption Rate in Tissue During Transurethral Prostatic Microwave Thermotherapy Using Heat Transfer Model," *IEEE Transactions on Biomedical Engineering*, **45**(9):1163–1172.
- Zhu, L., and Xu, L. X., 1999, "Evaluation of the Effectiveness of Transurethral Radio Frequency Hyperthermia in the Canine Prostate: Temperature Distribution Analysis," *ASME Journal of Biomechanical Engineering*, **121**(6):584–590.
- Zhu, L., He, Q., Xu, L. X., and Weinbaum, S., 2002, "A New Fundamental Bioheat Equation for Muscle Tissue: Part II—Temperature of SAV Vessels," *ASME Journal of Biomechanical Engineering*, in press.
- Zhu, L., Pang, L., and Xu, L. X., 2005, "Simultaneous Measurements of Local Tissue Temperature and Blood Perfusion Rate in the Canine Prostate during Radio Frequency Thermal Therapy," *Biomechanics and Modeling in Mechnobiology*, **4**(1):1–9.
- Zhu, L., Banerjee, R. K., Salloum, M., Bachmann, A. J., and Flower, R. W., 2008, "Temperature Distribution during ICG Dye-Enhanced Laser Photocoagulation of Feeder Vessels in Treatment of AMD-Related Choroidal Neovascularization (CNV). *ASME Journal of Biomechanical Engineering*, **130**(3):031010 (1–10).
- Zhu, L., Schappeler, T., Cordero-Tumangday, C., and Rosengart, A. J., 2009, "Thermal Interactions between Blood and Tissue: Development of a Theoretical Approach in Predicting Body Temperature during Blood Cooling/Rewarming," *Advances in Numerical Heat Transfer*, **3**:197–219.